



Fisheries New Zealand

Tini a Tangaroa

The 2017 stock assessment of paua (*Haliotis iris*) for PAU 5B

New Zealand Fisheries Assessment Report 2019/26

C. Marsh

ISSN 1179-5352

ISBN 978-0-9951270-6-7 (online)

July 2019



Requests for further copies should be directed to:

Publications Logistics Officer
Ministry for Primary Industries
PO Box 2526
WELLINGTON 6140

Email: brand@mpi.govt.nz
Telephone: 0800 00 83 33
Facsimile: 04-894 0300

This publication is also available on the Ministry for Primary Industries websites at:
<http://www.mpi.govt.nz/news-and-resources/publications>
<http://fs.fish.govt.nz> go to Document library/Research reports

© Crown Copyright – Fisheries New Zealand

TABLE OF CONTENTS

1. INTRODUCTION	2
1.1 Overview	2
1.2 Description of the fishery	2
2. MODEL	2
2.1 Changes since the 2013 assessment model of PAU 5B	3
2.2 Model description	3
2.2.1 Estimated parameters	4
2.2.2 Constants	5
2.2.3 Observations	5
2.2.4 Derived variables	6
2.2.5 Predictions	7
2.2.6 Initial conditions	7
2.2.7 Dynamics	8
2.2.8 Fitting	11
2.2.9 Fishery indicators	15
2.2.10 Markov chain-Monte Carlo (MCMC) procedures	15
2.2.11 Development of base case and sensitivity model runs	16
3. RESULTS	16
3.1 Preliminary model runs	16
3.2 MPD base case and sensitivity runs	18
3.3 MCMC results	18
3.3.1 Marginal posterior distributions and the Bayesian fit	19
3.3.2 Projections	19
4. DISCUSSION	20
5. ACKNOWLEDGMENTS	21
6. REFERENCES	21
A. APPENDIX A	50
GLOSSARY	51

EXECUTIVE SUMMARY

Marsh, C. (2019). The 2017 stock assessment of paua (*Haliotis iris*) for PAU 5B.

New Zealand Fisheries Assessment Report 2019/26. 52 p.

This report summarises the stock assessment for PAU 5B which included fishery data up to the 2016–17 fishing year. The report describes the model structure and output, including current (2017) and projected stock status. The stock assessment was implemented as a length-based Bayesian estimation model, with point estimates of parameters based on the mode of the joint posterior distribution, and uncertainty of model estimates investigated using the marginal posterior distributions generated from Markov chain Monte Carlo simulation.

The assessment showed that current and projected vulnerable biomasses were highly likely to stay above the target level (40% B_0). Spawning stock biomass was estimated to be above the hard and soft limits, with only one sensitivity run estimating a very low probability (less than 1%) of falling below the soft limit (20% B_0), under all projected scenarios.

The base case model estimated that the spawning stock in 2017 ($B_{current}$) was about 47% (95% CI 38–61%) of B_0 . Model projections were made under a range of future harvest level assumptions including current catch levels and increasing the TACC by 20%. Model projections also included two differing levels of future recruitment. Of these scenarios, future recruitment had a slightly larger impact on future stock status than the levels of exploitation explored. The base case model forecasted that the probability of the spawning stock biomass remaining above the target (40% B_0) by 2020 was greater than 85%.

The assessment model indicated that the stock status was very likely ($p = 93\%$) to be above the target, and that the estimated stock abundance has been increasing over recent years, corroborating the observed trend in the fishery. Results from sensitivity trials were close to the base case, and all estimated median stock status to be above the target. All runs considered in the assessment indicated that it was very unlikely the stock will fall below the soft or hard limits at current levels of catch.

1. INTRODUCTION

1.1 Overview

This report summarises the stock assessment model and outcomes for the PAU 5B (Stewart Island) stock with the inclusion of data to the end of the 2016–17 fishing year. The report describes the model structure and output, including current and projected stock status. The stock assessment was conducted with the length-based Bayesian estimation model first used in 1999 for PAU 5B (Breen et al. 2000a) with revisions made for subsequent assessments in PAU 5B (Breen et al. 2000b, Breen & Smith 2008a, Breen & Smith 2008b), PAU 4 (Breen & Kim 2004a), PAU 5A (Breen & Kim 2004b, Breen & Kim 2007, Fu & Mackenzie 2010a, b), PAU 5D (Breen et al. 2000a, Breen & Kim 2007), and PAU 7 (Andrew et al. 2000, Breen et al. 2001, Breen & Kim 2003, 2005, McKenzie & Smith 2009a, 2009b). PAU 5B was last assessed in 2013 (Fu 2014a and Fu et al. 2014a).

Seven sets of data were fitted in the assessment: (1) a standardised CPUE series covering 1990–2001 based on CELR data (CPUE), (2) a standardised CPUE series covering 2002–2017 based on PCELR data (PCPUE), (3) commercial catch sampling length frequency series (CSLF), (4) tag recapture length increment data, (5) maturity-at-length data, (6) research diver length frequency series (RDLF), and (7) research diver abundance survey index (RDSI). Catch history was an input to the model, encompassing commercial, recreational, customary, and illegal catch. Marsh et al. (2018) summarise the data input for this stock assessment.

The assessment was made in several steps. First, the model was fitted to the data with parameters estimated at the mode of their joint posterior distribution (MPD). Next, from the resulting fit, Markov chain-Monte Carlo (MCMC) simulations were made to obtain a large set of samples from the joint posterior distribution. From this set of samples, forward projections were made with a set of agreed indicators obtained. Sensitivity trials were explored by comparing MPD fits made with alternative model assumptions.

This document describes the model structure and assumptions, the fits to the data, estimates of parameters and indicators, and projection results. This report fulfils part of Objective 1 “Undertake a stock assessment for PAU 5B, using a length-based Bayesian model” for Ministry for Primary Industries Project PAU201701.

1.2 Description of the fishery

The paua fishery was summarised by Schiel (1992), and in numerous previous assessment documents (e.g., Schiel 1989, McShane et al. 1994, 1996, Breen et al. 2000a, 2000b, 2001, Breen & Kim 2003, 2004a, 2004b, 2007). A summary of the PAU 5B fishery up to the 2012–13 fishing year is presented in Marsh et al. (2018).

2. MODEL

This section gives an overview of the model used for the stock assessment of PAU 5B in 2017; for a full description see Breen et al. (2003). The model was developed for use in PAU 5B in 1999 and has been revised each year of subsequent assessments, in many cases echoing changes made to the rock lobster assessment model (Kim et al. 2004), which is a similar but more complex length-based Bayesian model. The last assessment completed using this model was for the paua stock PAU 5D (Marsh & Fu 2017), and this assessment builds on that model structure.

2.1 Changes since the 2013 assessment model of PAU 5B

A number of changes have been made to the stock assessment model since the last assessment of PAU 5B in 2013. One was to use a more flexible function form to describe the variance associated with the mean growth increment at length (See Section 2.2.7.2).

The predicted CPUE is now calculated after 50% of the fishing and natural mortality have occurred (previously the CPUE indices were fitted to the vulnerable biomass calculated after 50% of the catch was taken). This is considered to be appropriate if fishing occurs throughout a year (Schnute 1985). The change was recommended by the paua review workshop held in Wellington in March 2015 (Butterworth et al. 2015). Accordingly, mid-season numbers (and biomass) was calculated after half of the natural mortality and half of the fishing mortality was applied (See Section 2.2.7).

The third change was made to the likelihood function, fitting the tag-recapture observations so that weights could be assigned to individual observations (see Section 2.2.8.1); this also followed the paua review workshop's recommendation that "the tagging data should be weighted by the relative contribution of average yield from the different areas so that the estimates could better reflect the growth rates from the more productive areas" (Butterworth et al. 2015).

Two smaller changes were added in this iteration of the assessment model, including: 1) adding a lag between recruitment and spawning for models where the partition was started at more than 2 mm; and 2) adding a time varying parameter on the catchability coefficient on the CPUE observations (see Equations 23 and 26 for details on how this was applied).

2.2 Model description

The model partitioned the paua stock into a single sex population, with length classes from 70 mm to 170 mm, in groups of 2 mm (i.e., from 70 mm to less than 72 mm, 72 mm to less than 74 mm, etc.). In a separate run, the partition was started at 2 mm to test the sensitivity of the model to the assumption of the partition starting at 70 mm. The largest length bin was a plus group (170+ mm). The stock was assumed to be homogenous and reside in a single area. The partition accounted for numbers of paua by length class within an annual cycle, where movement between length classes was determined by estimated growth parameters. Paua entered the partition following a Beverton-Holt stock-recruitment relationship, and were removed by natural mortality and fishing mortality.

The model's annual cycle was based on the fishing year 1 October to 30 September, and these are referred to by the end year, e.g. fishing year 1998–99 (i.e., 1 October 1998 to 30 September 1999) is referred to as "1999". Any references to calendar years are denoted specifically.

The models were run for the years 1965–2017. The model assumed one time step within an annual cycle. Reported catches were used for 1974–2017, and those between 1965 and 1973 were assumed to increase linearly from 0 to the 1974 catch level. Catches included commercial, recreational, customary, and illegal catch, and all catches occurred at the same time.

Recruitment was assumed to take place at the beginning of the annual cycle, and length at recruitment was defined by a uniform distribution with a range between the first five length bins of the partition. Recruitment deviations (year class strengths) were assumed known, and equal to 1, for the years up to 1980. This was ten years before the length data were available (loosely based on the approximate time taken for recruited paua to appear on the right-hand side of the length distribution). The stock-recruitment relationship is unknown for paua, but is believed to be weak (Shepherd et al. 2001). A relationship may exist on small scales, but may not be apparent when large-scale data are modelled (Breen et al. 2003), following the assumption of a single homogenous stock in the model. This

assessment assumed a Beverton-Holt stock-recruitment relationship with a steepness (h) of 0.75 for the base case.

Maturity does not feature in the population partition. The model estimated proportion mature at each time step from length-at-maturity data. Growth and natural mortalities were also estimated within the model as time invariant parameters.

The model estimated two selectivities: the commercial fishing selectivity, and the Research Diver catch sample selectivity. Both selectivities had the option of following a logistic or double normal distribution (see 2.2.7.2).

The model was implemented in AD Model Builder™ (Otter Research Ltd., <http://otter-rsch.com/admodel.htm>) version 11.6, compiled with the MinGW 5.10 compiler.

2.2.1 Estimated parameters

Parameters estimated by the model were as follows. The parameter vector is referred to collectively as θ .

$\ln(R_0)$	natural logarithm of average recruitment under equilibrium conditions
M	instantaneous rate of natural mortality
g_1	expected annual growth increment at length L_1
g_2	expected annual growth increment at length L_2
ϕ	CV of the expected growth increment
α	one of two parameters that define the variance as a function of growth increment
β	one of two parameters that define the variance as a function of growth increment
Δ_{max}	maximum growth increment
l_{50}^g	length at which the annual increment is half the maximum
l_{95}^g	length at which the annual increment is 95% of the maximum
l_{95-50}^g	difference between l_{50}^g and l_{95}^g
q^I	catchability coefficient for the CPUE observation
q_{drift}^I	parameter for the CPUE observation that allows catchability to vary over the series
q^{I2}	catchability coefficient for the PCPUE observation
q_{drift}^{I2}	parameter for the PCPUE observation that allows catchability to vary over the series
q^{RDSI}	catchability coefficient for the RDSI observation
L_{50}	length at which maturity is 50%
L_{95-50}	interval between L_{50} and length at 95% selectivity
T_{50}	length at RDLF selectivity is 50%
T_{95-50}	difference between T_{50} and length at 95% selectivity
D_{50}	length at which commercial diver selectivity is 50%
D_{95-50}	difference between D_{50} and length at 95% selectivity
σ_{SR}	standard deviation for the right hand side of the double normal selectivity
σ_{SL}	standard deviation for the left hand side of the double normal selectivity
μ	the mean for the double normal selectivity
D^S	change in commercial diver selectivity for one unit change of MHS

$\tilde{\sigma}$	common component of error
\tilde{b}	shape parameter defining non-linearity between CPUE and biomass
$\boldsymbol{\varepsilon}$	vector of annual recruitment deviations, from 1980 to 2015
h	steepness of the Beverton-Holt stock-recruitment relationship
Δ_{max}	growth parameter in the inverse logistic formula

2.2.2 Constants

l_k	length of a paua at the midpoint of the k^{th} length class (l_k for class 1 is 71 mm, for class 2 is 73 mm and so on)
σ_{min}	minimum standard deviation of the expected growth increment (assumed to be 1 mm)
σ_{obs}	standard deviation of the observation error around the growth increment (assumed to be 0.25 mm)
MLS_t	minimum legal size in year t (assumed to be 125 mm for all years)
$P_{k,t}$	switch that describes whether abalone in the k^{th} length class in year t are above the minimum legal size (MLS) ($P_{k,t} = 1$) or below ($P_{k,t} = 0$)
a, b	constants for the length-weight relation, taken from Schiel & Breen (1991) (2.99×10^{-8} and 3.303 respectively, converting length in millimetres to weight in kilograms)
w_k	weight of an abalone at length l_k
ω^I	relative weight assigned to the CPUE dataset. This and the following relative weights were varied between runs to find a base case model run with balanced residuals
ω^{I2}	relative weight assigned to the PCPUE dataset
ω^S	relative weight assigned to CSLF dataset
ω^R	relative weight assigned to RDLF dataset
ω^{mat}	relative weight assigned to maturity-at-length data
ω^{tag}	relative weight assigned to tag-recapture data
ω_j^{tag}	relative weight assigned to tag-recapture observations that from area j
U^{max}	exploitation rate above which a limiting function was invoked (0.80 for the base case)
μ_ε	mean of the prior distribution for M
σ_M	assumed standard deviation of the prior distribution for M
σ_ε	assumed standard deviation of recruitment deviations in log space for years 1980–2012 (part of the prior for recruitment deviations)
n_ε	number of recruitment deviations
L_1	length associated with g_1 (75 mm)
L_2	length associated with g_2 (120 mm)
D_t^a	change in Minimum Harvest Size (MHS) in year t , (exogenous variable associated with the change in commercial diver selectivity in year t)
ssb_{lag}	spawning year related to the recruits entering the partition in a given year

2.2.3 Observations

C_t	observed catch in year t
I_t	standardised CPUE in year t
$I2_t$	standardised PCPUE in year t
σ_t^I	standard deviation of the estimate of observed CPUE in year t , obtained from the standardisation model

cv_t^I	CV of the estimate of observed CPUE in year t , obtained from the standardisation model
σ_t^{I2}	standard deviation of the estimate of observed PCPUE in year t , obtained from the standardisation model
cv_t^{I2}	CV of the estimate of observed PCPUE in year t , obtained from the standardisation model
$P_{k,t}^S$	observed proportion in the k^{th} length class in year t in CSLF
l_j	initial length for the j^{th} tag-recapture record
d_j	observed length increment of the j^{th} tag-recapture record
Δt_j	time at liberty for the j^{th} tag-recapture record
P_k^{mat}	observed proportion mature in the k^{th} length class in the maturity dataset

2.2.4 Derived variables

R_0	average number of annual recruits under equilibrium conditions
$N_{k,t}$	number of paua in the k^{th} length class at the start of year t
$N_{k,t+0.5}$	number of paua in the k^{th} length class in the mid-season of year t
$R_{k,t}$	recruits to the model in the k^{th} length class in year t
g_k	expected annual growth increment for paua in the k^{th} length class
σ^{gk}	standard deviation of the expected growth increment for paua in the k^{th} length class, used in calculating G
G	growth transition matrix
B_t	spawning stock biomass at the beginning of year t
$B_{t+0.5}$	spawning stock biomass in the mid-season of year t
B_0	spawning stock biomass assuming population in an equilibrium state.
B_t^r	biomass of paua above the MLS at the beginning of year t
$B_{t+0.5}^r$	biomass of paua above the MLS in the mid-season of year t
B_0^r	equilibrium biomass of paua above the MLS assuming no fishing and average recruitment from the period in which recruitment deviations were estimated
B_t^v	vulnerable (to commercial fishing) biomass of paua at the beginning of year t
U_t	exploitation rate in year t
A_t	the complement of exploitation rate
$SF_{k,t}$	finite rate of survival from fishing for paua in the k^{th} length class in year t
V_k^k	relative selectivity of commercial divers for paua in the k^{th} length class
$\sigma_{k,t}^S$	error of the predicted proportion in the k^{th} length class in year t in CSLF data
n_t^S	relative weight (effective sample size) of the CSLF data in year t
σ_j^d	standard deviation of the predicted length increment for the j^{th} tag-recapture record
σ_j^{tag}	total error predicted for the j^{th} tag-recapture record
σ_k^{mat}	error of the proportion mature-at-length for the k^{th} length class
\tilde{q}_t^I	scalar for between biomass and CPUE observation
\tilde{q}_t^{I2}	scalar for between biomass and PCPUE observation
\tilde{q}_t^{I2}	scalar for between biomass and PCPUE observation
$-\ln(L)$	negative log-likelihood
f	total function value

2.2.5 Predictions

\hat{l}_t	predicted CPUE in year t
$\hat{l}2_t$	predicted PCPUE in year t
$\hat{p}_{k,t}^r$	predicted proportion in the k^{th} length class in Research Diver LF
$\hat{p}_{k,t}^s$	predicted proportion in the k^{th} length class in year t in commercial catch sampling
\hat{d}_j	predicted length increment of the j^{th} tag-recapture record
\hat{p}_k^{mat}	predicted proportion mature in the k^{th} length class

2.2.6 Initial conditions

The initial population was assumed to be in equilibrium with zero fishing mortality and the base recruitment (R_0). The model was run for 60 years with no fishing to obtain near-equilibrium in numbers-at-length. Recruitment was evenly divided among the first five length bins:

- (1) $R_{k,t} = 0.2R_0$ for $1 \leq k \leq 5$
- (2) $R_{k,t} = 0$ for $k > 5$

A growth transition matrix was calculated inside the model from the estimated growth parameters. Three growth models were explored to describe mean annual growth increment for k^{th} length class (Δl_k). The three models were the exponential, the inverse logistic and the linear growth models. The inverse logistic model was chosen as providing the best fit with the expected annual growth increment for the k^{th} length class being:

$$(3) \quad \Delta l_k = \frac{\Delta_{max}}{1 + \exp(\ln(19) \left(\frac{l_k - l_{50}^g}{l_{95}^g - l_{50}^g} \right))}$$

For comparison, if the exponential growth model had been applied, the expected annual growth increment for the k^{th} length class would have been:

$$(4) \quad \Delta l_k = g_1 (g_2/g_1)^{(l_k - L_1)/(L_2 - L_1)}$$

And if the linear growth model was applied, the expected annual growth increment for the k^{th} length class would have been:

$$(5) \quad \Delta l_k = \left(\frac{L_2 g_1 - L_1 g_2}{g_1 - g_2} - l_k \right) \left[1 - \left(1 + \frac{g_1 - g_2}{L_1 - L_2} \right) \right]$$

The model used the AD Model Builder™ function *posfun*, with a dummy penalty, to ensure a positive expected increment at all lengths, using a smooth differentiable function.

The standard deviation of Δl_k was assumed to be proportional to Δl_k with minimum σ_{min} :

$$(6) \quad \sigma^{\Delta l_k} = (\Delta l_k \phi - \sigma_{min}) \left(\frac{1}{\pi} \tan^{-1}(10^6(\alpha \Delta l_k \phi - \sigma_{min})) + 0.5 \right) + \sigma_{min}$$

Or a more complex functional form between the growth increment and its standard deviation defined as:

$$(7) \quad \sigma^{\Delta l_k} = (\alpha(\Delta l_k)^\beta - \sigma_{min}) \left(\frac{1}{\pi} \tan^{-1} \left(10^6 (\alpha(\Delta l_k)^\beta - \sigma_{min}) \right) + 0.5 \right) + \sigma_{min}$$

From the expected increment and standard deviation for each length class, the probability distribution of growth increments for a paua of length l_k was calculated from the normal distribution and translated into the vector of probabilities of transition from the k^{th} length bin to other length bins to form the growth transition matrix \mathbf{G} . Zero and negative growth increments were permitted, i.e., the probability of staying in the same bin or moving to a smaller bin could be non-zero.

In the initialisation, the vector \mathbf{N}_t of numbers-at-length was determined from numbers in the previous year, survival from natural mortality, the growth transition matrix \mathbf{G} , and the vector of recruitment \mathbf{R}_t :

$$(8) \quad \mathbf{N}_t = (\mathbf{N}_{t-1} e^{-M}) \bullet \mathbf{G} + \mathbf{R}_t$$

where the dot (\bullet) denotes matrix multiplication.

2.2.7 Dynamics

2.2.7.1 Sequence of operations

After initialisation, the first model year was 1965 and the model was run through to 2017. In the first nine years the model was run with an assumed catch vector, because it was unrealistic to assume that the fishery was in a virgin state when the first catch data became available in 1974. The assumed catch vector increased linearly from zero to the 1974 catch. These years can be thought of as an additional part of the initialisation, but they use the dynamics described in this section.

Model dynamics were sequenced as follows:

- Numbers at the beginning of year $t-1$ were subjected to fishing, followed by natural mortality, then growth, to produce the numbers at the beginning of year t .
- Recruitment was added to the numbers at the beginning of year t .
- Biomass available to the fishery was calculated and, with catch, was used to calculate the exploitation rate, which was constrained if necessary.
- Half the exploitation rate and half natural mortality were applied to obtain mid-season numbers, from which the predicted abundance indices and proportions-at-length were calculated. Mid-season numbers were not used further.

2.2.7.2 Main dynamics

For each year t , the model calculated the start-of-the-year biomass available to the commercial fishery. Due to voluntary changes in harvest size from fishers, a time varied selectivity was applied based on an exogenous variable. Biomass available to the commercial fishery was:

$$(9) \quad B_t^v = \sum_k N_{k,t} V_k^S W_k$$

$$(10) \quad V_k^{t,S} = \frac{1}{1 + 19 \left(\frac{(l_k - D_{50})}{D_{95-50}} \right)} \quad \text{for } t < 2006 \text{ assuming logistic selectivity}$$

$$(11) \quad V_k^{t,S} = \frac{1}{1+19 \left(\frac{(l_k - D_{50} - D_t^a D^S)}{D_{95-50}} \right)} \quad \text{for } t \geq 2006 \text{ assuming logistic selectivity}$$

$$(12) \quad V_k^{t,S} = \begin{cases} 2^{-\left[\frac{(l_k - \mu)}{\sigma_{SL}}\right]^2} & (l_k \leq \mu) \\ 2^{-\left[\frac{(l_k - \mu)}{\sigma_{SR}}\right]^2} & (l_k > \mu) \end{cases} \quad \text{for } t < 2006 \text{ assuming double normal selectivity}$$

$$(13) \quad V_k^{t,S} = \begin{cases} 2^{-\left[\frac{(l_k - \mu - D_t^a D^S)}{\sigma_{SL}}\right]^2} & (l_k \leq \mu) \\ 2^{-\left[\frac{(l_k - \mu - D_t^a D^S)}{\sigma_{SR}}\right]^2} & (l_k > \mu) \end{cases} \quad \text{for } t \geq 2006 \text{ assuming double normal selectivity}$$

This model had the option of two selectivities for the fishery; either the logistic (Equations 10 and 11) or the double normal (Equations 12 and 13). The observed catch was then used to calculate the exploitation rate ($U_t = C_t / B_t^v$). Survival rate (Equation 14) was constrained by A_{min} (where $A_{min} = 1 - U^{max}$) using ADMB's posfun function (Equation 15). If the ratio of catch to vulnerable biomass exceeded U^{max} , then survival rate was constrained and a penalty was added to the total negative log-likelihood function (Equation 16).

$$(14) \quad A_t = 1 - U_t \quad \text{for } \frac{C_t}{B_t^v} \leq U^{max}$$

$$(15) \quad A_t = A_{min} / \left(2 - \frac{\left(1 - \frac{C_t}{B_t^v}\right)}{A_{min}} \right) \quad \text{for } \frac{C_t}{B_t^v} > U^{max}$$

The penalty invoked when the exploitation rate exceeded U^{max} was:

$$(16) \quad 10000000 \left(A_{min} - \left(1 - \frac{C_t}{B_t^v} \right) \right)^2$$

This prevented the model from exploring parameter combinations that gave unrealistically high exploitation rates. Survival from fishing was calculated as:

$$(17) \quad SF_{k,t} = 1 - (1 - A_t)P_{k,t}$$

or

$$(18) \quad SF_{k,t} = 1 - (1 - A_t)V_k^S$$

The vector of numbers-at-length in year t was calculated from numbers in the previous year:

$$(19) \quad \mathbf{N}_t = \left((\mathbf{S}\mathbf{F}_{t-1} \otimes \mathbf{N}_{t-1}) e^{-M} \right) \bullet \mathbf{G} + \mathbf{R}_t$$

where \otimes denotes the element-by-element vector product. The vector of recruitment, \mathbf{R}_t , was determined from R_0 , estimated recruitment deviations, and the stock-recruitment relationship:

$$(20) \quad R_{k,t} = 0.2 R_0 e^{(\varepsilon_t - 0.5\sigma^2)} \frac{B_{t-ssb_{lag}+0.5}}{B_0} / \left[1 - \frac{5h-1}{4h} \left[1 - \frac{B_{t-ssb_{lag}+0.5}}{B_0} \right] \right] \quad \text{for } 1 \leq k \leq 5$$

$$(21) \quad R_{k,t} = 0 \quad \text{for } k > 5$$

The recruitment deviation parameters ε_t were estimated for all years from 1980. The recruitment deviations were constrained to have a mean of 1 in arithmetic space. ssb_{lag} was an offset added in this assessment round that allowed a lag between spawning and when recruits enter the partition (usually 70 mm).

The model predicted CPUE in year t from mid-season recruited biomass, the scaling coefficient, and the shape parameter:

$$(22) \quad \hat{I}_t^l = \tilde{q}_t^l (B_{t+0.5}^v)^{\tilde{b}}$$

$$(23) \quad \tilde{q}_t^l = \begin{cases} q^l, & t = 1 \\ q_{t-1}^l * (1 + q_{drift}^l), & t > 1 \end{cases}$$

Available biomass $B_{t+0.5}^v$ was the mid-season vulnerable biomass after half the catch had been removed and half natural mortality applied (because the catch occurred throughout the fishing year). It was calculated as in Equation 9, but using the mid-year numbers $N_{t+0.5}$:

$$(24) \quad N_{t+0.5} = N_t \exp(-0.5M) \left(1 - \frac{(1-A_t)}{2} V_t^s \right)$$

Similarly,

$$(25) \quad \hat{I}_t^{l2} = \tilde{q}_t^{l2} (B_{t+0.5}^v)^{\tilde{b}}$$

where the same shape parameter \tilde{b} was used for both the early and recent CPUE series and where:

$$(26) \quad \tilde{q}_t^{l2} = \begin{cases} q^{l2}, & t = 1 \\ q_{t-1}^{l2} * (1 + q_{drift}^{l2}), & t > 1 \end{cases}$$

The Research Diver LF selectivity V_k^r was calculated from:

$$(27) \quad V_k^r = \frac{1}{1 + 19^{-\left(\frac{(l_k - T_{50})}{T_{95-50}}\right)}}$$

The model predicted proportions-at-length for the CSLF from numbers in each length class for lengths greater than 116 mm:

$$(28) \quad \hat{P}_{k,t}^s = \frac{N_{k,t+0.5} V_{k,t}^s}{\sum_{k=23}^{51} N_{k,t+0.5} V_{k,t}^s}$$

Predicted proportions-at-length for RDLF were similar:

$$(29) \quad \hat{P}_{k,t}^F = \frac{N_{k,t+0.5} V_{k,t}^F}{\sum_{k=25}^{51} N_{k,t+0.5} V_{k,t}^F}$$

The predicted increment for the j^{th} tag-recapture record for a yearly time period, using the inverse-logistic model, was:

$$(30) \quad \hat{d}_j = \Delta t_j \frac{\Delta_{max}}{\left(1 + \exp\left(\frac{\ln(19)(l_j - l_{50}^g)}{(l_{95}^g - l_{50}^g)}\right)\right)}$$

where Δt_j is the time at liberty (proportion of a year). This allowed observations that were not at liberty for exactly a year to be fitted without being considered outliers. For example, if we recaptured an individual halfway through the year (days at liberty = 178), $\Delta t_j = 0.5$. This assumes that growth is uniform throughout the year. This assumption is not considered that important because the tag-recapture studies are designed to target tags at liberty for a year, and so there are not many recaptures that deviate drastically from a year at liberty. For the exponential model the expected increment was:

$$(31) \quad \hat{d}_j = \Delta t_j g_\alpha (g_\beta / g_\alpha)^{(L_j - \alpha) / (\beta - \alpha)}$$

The error around an expected increment was:

$$(32) \quad \sigma_j^d = \left(\alpha (\hat{d}_j)^\beta - \sigma_{min} \right) \left(\frac{1}{\pi} \tan^{-1} \left(10^6 \left(\alpha (\hat{d}_j)^\beta - \sigma_{min} \right) \right) + 0.5 \right) + \sigma_{min}$$

Predicted maturity-at-length was:

$$(33) \quad \hat{p}_k^{mat} = \frac{1}{1 + 19^{-\left((l_k - L_{50}) / L_{95-50} \right)}}$$

2.2.8 Fitting

2.2.8.1 Likelihoods

The distribution of CPUE was assumed to be normal-log and the negative log-likelihood was:

$$(34) \quad -\ln(\mathbf{L}) (\hat{l}_t | \theta) = \frac{(\ln(l_t) - \ln(\hat{l}_t))}{2 \left(\frac{\sigma_t^l \tilde{\sigma}}{\varpi^l} \right)} + \ln \left(\frac{\sigma_t^l \tilde{\sigma}}{\varpi^l} \right) + 0.5 \ln(2\pi)$$

where

$$(35) \quad \sigma_t^l = \sqrt{\ln((cv_t^l)^2 + 1)}$$

and similarly for PCPUE:

$$(36) \quad -\ln(\mathbf{L}) (\hat{l}_{2t} | \theta) = \frac{(\ln(l_{2t}) - \ln(\hat{l}_{2t}))}{2 \left(\frac{\sigma_t^{l2} \tilde{\sigma}}{\varpi^{l2}} \right)} + \ln \left(\frac{\sigma_t^{l2} \tilde{\sigma}}{\varpi^{l2}} \right) + 0.5 \ln(2\pi)$$

where

$$(37) \quad \sigma_t^{I2} = \sqrt{\ln((cv_t^{I2})^2 + 1)}$$

The proportions-at-length from CSLF data are assumed to follow a multinomial distribution, with a standard deviation that depends on the effective sample size and the weight assigned to the data:

$$(38) \quad \sigma_{k,t}^s = \frac{\tilde{\sigma}}{\omega^s n_t^s}$$

The negative log-likelihood was:

$$(39) \quad -\ln(L) (\hat{P}_{k,t}^s | \theta) = \frac{P_{k,t}^s}{\sigma_{k,t}^s} \left(\ln(P_{k,t}^s + 0.01) - \ln(\hat{P}_{k,t}^s + 0.01) \right)$$

Errors in the tag-recapture dataset were also assumed to be normal. For the j^{th} record, the total error is a function of the predicted standard deviation (Equation 38), observation error, and weight assigned to the data:

$$(40) \quad \sigma_j^{tag} = \tilde{\sigma} / \omega^{tag} \sqrt{\sigma_{obs}^2 + (\sigma_j^d)^2}$$

The negative log-likelihood for an observation is:

$$(41) \quad -\ln(L) (\hat{d}_j | \theta) = \omega_g^{tag} \left(\frac{(d_j - \hat{d}_j)^2}{2(\sigma_j^{tag})^2} + \ln(\sigma_j^{tag})^2 + 0.5 \ln(2\pi) \right)$$

where ω_g^{tag} is a weighting factor calculated as:

$$(42) \quad \omega_g' = p_g \frac{n_g}{\sum_g n_g}$$

$$(43) \quad \bar{\omega} = \frac{\sum_g \omega_g'}{G}$$

$$(44) \quad \omega_g^{tag} = \omega_g' / \bar{\omega}$$

where p_g is the proportion of catch from area g (where the observation is made), n_g is the number of tag-recapture observations from area. This addresses the suggestion from the review (Butterworth et al. 2015), that tag data should be weighted by catch so that growth models were representative of the commercial fishery. This method also allows for the consideration of weighting the area by the number of observations within each area. ω_g^{tag} can be fixed at 1 if the likelihood is not to be weighted.

The proportion mature-at-length was assumed to be normally distributed, with standard deviation analogous to proportions-at-length:

$$(45) \quad \sigma_k^{mat} = \frac{\tilde{\sigma}}{\omega^{mat} \sqrt{P_k^{mat} + 0.1}}$$

The negative log-likelihood was:

$$(46) \quad -\ln(\mathbf{L}) (\hat{P}_k^{mat} | \theta) = \frac{(P_k^{mat} - \hat{P}_k^{mat})^2}{2(\sigma_k^{mat})^2} + \ln(\sigma_k^{mat}) + 0.5\ln(2\pi)$$

2.2.8.2 Normalised residuals

These are calculated as the residual divided by the relevant σ term used in the likelihood. For CPUE, the normalised residual was:

$$(47) \quad \frac{\ln(I_t) - \ln(\hat{I}_t)}{\left(\frac{\sigma_t^I \bar{\sigma}}{\omega^I}\right)}$$

and similarly for PCPUE. For the CSLF proportions-at-length, the residual was:

$$(48) \quad \frac{P_{k,t}^S - \hat{P}_{k,t}^S}{\sigma_{k,t}^S}$$

For tag-recapture data, the residual was:

$$(49) \quad \frac{d_j - \hat{d}_j}{\sigma_j^{tag}}$$

and for the maturity-at-length data the residual was:

$$(50) \quad \frac{P_k^{mat} - \hat{P}_k^{mat}}{\sigma_k^{mat}}$$

2.2.8.3 Dataset weights

Proportions-at-length (CSLF and RDLF) were included in the model with a multinomial likelihood. The length frequencies for individual years were assigned relative weights (effective sample size), based on a sample size that represented the best least squares fit of $\log(cv_i) \sim \log(P_i)$, where cv_i was the bootstrap CV for the i th proportion, P_i (See Figure A1, Appendix A, for a plot of this relationship). The weights for individual years (n_t^S for CSLF and n_t^R for RDLF) were multiplied by the weight assigned to the dataset (ω^S for CSLF and ω^R for RDLF) to obtain the model weights for the observations. We used the weighting scheme following Francis (2011) for the base case model, where the weight for the CSLF dataset was determined as:

$$(51) \quad \omega^S = 1/\text{var}_t[(\bar{O}_t^S - \bar{E}_t^S)/(v_t^S/n_t^S)^{0.5}] \quad (\text{Method TA1.8, table A1 in Francis 2011})$$

where

$$(52) \quad \bar{O}_t^S = \sum_k p_{k,t}^S l_k$$

$$(53) \quad \bar{E}_t^S = \sum_k \hat{p}_{k,t}^S l_k$$

$$(54) \quad V_t^S = \sum_k l_k^2 \hat{P}_{k,t}^S - (\bar{E}_t^S)^2$$

The TA1.8 method allows for the possibility of substantial correlations within a dataset, and generally produces relatively small sample sizes, thus down-weighting the composition data (Francis 2011). The actual and estimated sample sizes for the commercial catch at length using the two methods are given in Table 1.

The relative abundance indices (CPUE and PCPUE) were included in the model with a lognormal likelihood. In previous assessments, the weight of the abundance datasets was determined iteratively so that the standard deviation of the normalised residuals was close to one. In this assessment, we used a weighting scheme recommended by Francis (2011), with a small modification recommended by the review workshop (Butterworth et al. 2015). With this approach, a series of loess lines of various degrees of smoothing were fitted to the abundance indices (this was carried out outside the assessment model), and the CV was calculated using the residuals from the loess line which was considered to have the "appropriate" smoothness. This CV was then adjusted for the degrees of freedom associated with the smoothing:

$$(55) \quad \tilde{cv} = cv \left(\frac{n}{n-d} \right)$$

Where CV was calculated using the residuals, n was the number of indices, d was degree of freedom, and \tilde{cv} was the adjusted value. The adjusted CV was applied to all years in the time series and remained constant in the stock assessment model. The choice of the "appropriate" fit was based on visual examination of the loess lines, by the SFWG.

For the early CPUE (1990–2001), the residuals from the loess line which had the "appropriate" smoothness ($df=5$) had an adjusted CV of 0.09 (Figure A1, top left, Appendix A); for the recent CPUE (2002–2017), a CV of 0.1 was considered to be appropriate ($df=5$, Figure A1, top right, Appendix A), for the combined series a CV was chosen (Figure A2, bottom left, Appendix A). The CVs of the CPUE observations in the assessment model were fixed at those values (except for sensitivity runs in which alternative values were assumed).

2.2.8.4 Priors and bounds

Bayesian priors were established for all estimated parameters (Table 2). Most had uniform (uninformed) distributions with upper and lower bounds initially set arbitrarily wide so as not to constrain the estimation. Recent research has demonstrated the dangers of setting upper limits too high on parameters such as $\ln(R_0)$ with assumed uniform priors in data limited assessments (Thorson & Cope 2017). For this reason, sensitivity runs were done on the upper bound of the $\ln(R_0)$. The prior probability density for M was assumed to be uniform.

The prior probability density for the vector of estimated recruitment, was assumed to be normal with a mean of zero and a standard deviation (σ_ϵ). The contribution to the objective function for the whole vector is:

$$(56) \quad -\ln(\mathbf{L}) (\epsilon | \mu_\epsilon, \sigma_\epsilon) = \frac{\sum_{i=1}^{n_\epsilon} (\epsilon_i)^2}{2(\sigma_\epsilon)^2} + \ln(\sigma_\epsilon) + 0.5\ln(2\pi)$$

2.2.8.5 Penalty

A penalty was applied to exploitation rates higher than the assumed maximum (Equation 16). The penalty was added to the objective function after being multiplied by an arbitrary weight (1000000).

AD Model Builder™ also has internal penalties that keep estimated parameters within their specified bounds, but these were expected to have no effect on the outcome as the choice of a base case excluded situations where parameters were estimated at or near a bound.

2.2.9 Fishery indicators

The assessment calculated the following quantities from their posterior distributions of the model's mid-season spawning and recruited biomass for 2017 ($B_{current}$ and $B_{current}^r$) and for the projection period (B_{proj} and B_{proj}^r).

Simulations were carried out to calculate deterministic MSY, the maximum constant annual catch that can be sustained under deterministic recruitment. A single simulation run was done by starting from an unfished equilibrium state, and running under a constant exploitation rate until the catch and spawning stock biomass stabilised. For each simulation run with exploitation rate U , the equilibrium total annual catch and spawning stock biomass were calculated. The exploitation rate U that maximized the annual catch was U_{msy} . The corresponding catch was MSY, and the corresponding SSB was B_{msy} . Together with B_0 , B_{msy} , $U_{current}$, U_{40B_0} and U_{msy} the current and projected stock status was reported in relation to the following indicators:

$\%B_0$	current and projected spawning biomass as a percent of B_0 ,
$\%B_{msy}$	current and projected spawning biomass as a percent of B_{msy}
$Pr(> B_{current})$	probability that current and projected spawning biomass is greater than $B_{current}$
$Pr(> B_{msy})$	probability that current and projected spawning biomass is greater than B_{msy}
$\%B_0^r$	current and projected recruited biomass as a percent of B_0^r
$\%B_{msy}^r$	current and projected recruited biomass as a percent of B_{msy}^r
$Pr(> B_{msy}^r)$	probability that current and projected recruit-sized biomass is greater than B_{msy}^r
$Pr(> B_{current}^r)$	probability that projected recruit-sized biomass is greater than $B_{current}^r$
$Pr(B_{proj} > 40\%B_0)$	probability that current and projected spawning biomass is greater than 40% B_0
$Pr(B_{proj} < 20\%B_0)$	probability that current and projected spawning biomass is less than 20% B_0
$Pr(B_{proj} < 10\%B_0)$	probability that current and projected spawning biomass is less than 10% B_0
$Pr(U_{proj} > U_{40\%B_0})$	probability that current and projected exploitation rate is greater than U_{40B_0}

2.2.10 Markov chain-Monte Carlo (MCMC) procedures

AD Model Builder™ uses the Metropolis-Hastings algorithm to conduct (Markov chain-Monte Carlo) MCMC. The step size was based on the standard errors of the parameters and their covariance relationships, estimated from the Hessian matrix.

For the MCMCs in this assessment, single long chains were run, starting at the MPD estimate. The base case was 5 million simulations, from which every 5000th sample was saved. The value of $\tilde{\sigma}$ was fixed to that used in the MPD run because it was considered inappropriate to let a variance component change during the MCMC.

2.2.11 Development of base case and sensitivity model runs

The 2017 base case was developed from the base case used in the last accepted assessment for PAU 5B (Fu 2014a), and incorporated several changes as described in Section 2.1. The 2017 base case was tested for consistency with the 2013 base case by running it with the same data. The 2017 base case produced a similar fit and relative trend to that produced from the 2013 assessment base case, but with a slightly higher biomass (Figure 1).

The Shellfish Working Group (SFWG) then requested an ensemble of initial model runs to be conducted. The initial model runs investigated aspects of model configurations such as data weighting methods, choice of growth model, and the inclusion of alternative CPUE indices and catch histories. The results of the initial model runs are briefly summarised in Section 3.1. For a summary of parameters that were fixed across all model runs see Table 3. The configurations of the initial model runs are summarised in Table 4. After reviewing the diagnostics and outputs from the initial model runs (Section 3.1), the SFWG requested one base case model run, and a suite of sensitivity model runs. The sensitivity model runs encompassed model uncertainty, whilst still being biologically plausible.

3. RESULTS

3.1 Preliminary model runs

Initial model runs considered a large range of model configurations, which generated candidate models for the base case and sensitivities runs. Key conclusions drawn from the initial diagnostics are summarised below:

- The major model structure change since the last assessment was based on the assumption that half of the fishing and natural mortality had occurred prior to calculating CPUE fits. This appeared to have little effect on the model fits and derived quantities, but resulted in slightly higher equilibrium biomass estimates (Figure 1).
- The weighting of tag-recapture observations by stratum, catch and number of observations had very little effect on model quantities (Figure 4). This is thought to be due to there being little variation in catch from strata where tag-recaptures were observed.
- Investigating hyperdepletion and hyperstability scenarios with the shape parameter (\tilde{b}) on CPUE. Initially \tilde{b} was estimated, with a uniform prior bounded between 0.5 and 1.5. The initial estimate ran to the lower bound. A profile was run over the parameter space, which was flat. As a sensitivity analysis, two runs were presented at the upper and lower bounds. These generated different fits to CPUE (Figure 2) and generated the largest divergence in stock status in the initial investigation (Figure 3).
- Including the RDLF and RDSI data had little influence, while the model run including the research diver information lowered the absolute biomass slightly, but kept a similar trajectory (Figure 5). This was caused by a slightly different fit to the first CPUE series (Figure 6), suggesting that the research diver information had a signal for greater exploitation during that

period. This sensitivity was explored because there has been considerable historical debate over whether research diver information should be included. It has been agreed that this data is not representative (Haist 2010) and also that there may be nonlinear relationships between abundance and observations (Cordue 2009).

- The exponential and inverse-logistic growth model were both explored. The inverse logistic gave a larger absolute biomass with a higher B_0 by about 1000 t (Figure 7), but similar relative biomass trends. The inverse logistic growth model yielded a slightly ‘better’ visual fit to length frequency data (Figure 8).
- Alternative values for the variance prior on the recruitment deviations were investigated. There is little information on the variability of recruitment of paua at a Quota Management Area level. Alternative values of recruitment variability for the recruitment deviation priors were 0.2 and 0.6. There was little difference between the model fits and quantities with different prior variances.
- Changing the lag of spawning to recruitment had little effect on the model outcome. It was observed that the estimates of the recruitment deviations were changed as the spawning lag changed, resulting in very similar levels of recruitment for each year (Figure 9). A spawning lag of three years was used as a default. This was based on the approximate time it is assumed that an average individual takes to reach 70 mm.
- The model fits and quantities were not affected by changing the partition start length from 70 mm to 2 mm (Figure 10).
- Additional error was added to the CPUE of both series to investigate the effect of having less precise relative biomass indices. The fit to both series was very similar between the models with CV of 10% and models with an additional 20% process error resulting in CVs of 37% (Figure 11).
- A component of uncertainty in the PAU 5 stock regions is the historical catch histories. These were defined in Marsh et al. (2018) and tested as initial sensitivity runs, which changed the absolute scale of the stock size but did not affect model fits.
- Recent research has suggested that the estimate of log (ln) transformed parameters with uniform priors in data ‘limited’ assessments is sensitive to the value of the upper bound (Thorson & Cope 2017). This was explored with a range of arbitrarily chosen values for the upper bound. The model estimated identical parameter estimates for all values.
- The final model sensitivity run allowed for the catchability parameter to change over time according to Equation 12. This was applied to the combined CPUE series, where the drift parameter was estimated with a uniform prior bounded between -0.05 and 0.05 (see Figure 12 to compare derived SSBs under this assumption).
- Other runs that were explored but not included in this summary included alternative values for the exogenous selectivity variable, combined CPUE series, assuming an informative prior on natural mortality, different commercial catch histories, bounds on parameter estimates specifically $\ln R_0$ and different combinations of the above settings. These model runs were not included in this report as any resulting differences in fits and model quantities were minor.

3.2 MPD base case and sensitivity runs

The configurations of the base case model (0.1) and the six sensitivity runs (0.1all and 0.2-0.6) are listed in Table 4. MPD estimates of objective function values (negative log-likelihood), parameters, and indicators for the base case and sensitivity runs are summarised in Table 5. The suite of models considered for MCMC estimation were: the two CPUE series (0.2), excluding research diver observations (0.3), alternative catch history (0.4), modelling the partition at 2 mm (0.5), and estimating a time varying catchability (0.6).

The base case model predicted the main trends in the CPUE series well, and most fits were within the confidence bounds of the observed values, except for the years 2009 and 2010 of the series (Figure 13).

Commercial catch length frequencies were well-fitted for most years (Figure 14). The mean length of CSLF increased between 2007 and 2016 (Figure 15), due to the voluntary change in MHS that has occurred in the fishery. The effect of this can be observed in the estimated selectivity (Figure 16). The standardised residuals of the fits to CSLF revealed that most of the difficulty in fits came around a50-a95 (Figure 14). This is due to the steep knife edge like selectivity around the MHS, i.e., if the exogenous variable is off slightly for a given year this causes a misfit and is why the main residual patterns occur around the MHS size.

The fits to the other data sets (RDLF, RDSI, tag recapture data and maturity at length data) were all deemed satisfactory by the SFWG (Figures 17–18).

Sensitivity runs, selected by the SFWG from the initial model runs, tested a set of components that encompassed most of the uncertainty whilst being biologically plausible. These components included removing the RDLF and RDSI data sets, fitting to the CPUE series as two separate series instead of the base case of a combined index of abundance, alternative commercial catch history, beginning the partition at 2 mm, and estimating a time-varying drift catchability coefficient. The range of biomass trajectories from all these sensitivity runs is shown in Figure 19.

There was little difference between sensitivity runs and the base case chosen by the SFWG. The model with the lowest stock status was model 0.6 with the time varying catchability, with a current stock status of 39.8% B_0 . The other sensitivities and base case had current stock status between 45 and 47 % B_0 .

Late in the assessment process, CSLF data for the 2017 fishing year became available. This was added into the base case model as a sensitivity run (0.1 all CSLF) to see if there were any consequences of leaving this data out of the base case model. Including the 2017 data made no change to model fits and quantities (Figures 20-21).

All the sensitivity runs were taken to MCMC to assess marginal posteriors and uncertainty.

3.3 MCMC results

The SFWG requested that model runs 0.1, 0.2, 0.3, 0.4, 0.5 and 0.6 be estimated by MCMC, to derive the posterior distributions of estimated parameters and biomass indicators. Only results from model runs 0.1, 0.4 and 0.6 are discussed in later sections. This was because model runs 0.2, 0.3 and 0.5 had very similar posterior fits and quantities to the base case model (0.1).

All MCMC chains were diagnosed for convergence by visually assessing trace plots of the objective function and key parameters. The traces of key indicators (B_0 and $B_{current}$) across most chains showed no visual evidence of non-convergence (Figure 22).

3.3.1 Marginal posterior distributions and the Bayesian fit

The base case model marginal posterior fits to all data sources are shown in Figures 23–27. These were deemed adequate fits by the SFWG. On average the base case model tracked most trends in all the datasets well. The model struggled to fit the plus group in the earlier CSLF data (Figure 24), but obtained a good fit to the RDLF data. This suggested a slight conflict between these two data sources that couldn't be resolved. This conflict was relatively minor and accepted by the SFWG. The RDSI was generally well fit apart from the year 1994, where the model could not predict such a high biomass.

Model quantities showed that the current spawning population had a high probability (93%) of being above the target limit, based on the base case model. This follows a decline during the 1980s and 1990s and an increase during the 2000s (Figure 28). The SSB trajectory has flattened off over the past five years which is due to lower than average recruitment (Figure 29).

The sensitivity run that had an alternative commercial catch history (run 0.4) had a very similar fit to the base case model and similar relative model quantities, but with a higher absolute SSB (Figure 30), with a median B_0 of 4469 t compared to 3948 in the base case model.

The final sensitivity run, estimating a time varying catchability coefficient, expressed the largest uncertainty in spawning stock size. The visual inspection of the trace plot showed no departure from a stationarity distribution and, while the model quantities were much more variable than the other two runs (Figure 31), the fits were very similar to those seen in models 0.1 and 0.4, with similar trends being observed.

Overall, the three models taken to MCMC generated very similar fits to the observations and model quantities. All models expressed the decline in SSB to the early 2000s followed by a recovery. The period of the recovery followed a TACC increase and above average year class strengths, which has since shifted to below average recruitment in the past four years.

3.3.2 Projections

Three-year projections (2018–2020) were carried out for the three model runs taken to MCMC (0.1, 0.4, and 0.6).

For each model, eight future scenarios were run, including alternative recruitment assumptions and alternative future harvest levels. The future recruitment was applied by empirical resampling with equal probability from the MCMC sample estimates. This method assumes that future recruitment follows that estimated for the resampled period. Two time periods were used for resampling, the past ten years (2005–2015) and the past five years (2011–2015). Traditionally the period of recruitment resampling is from the past ten-year of estimates. The five year scenario was explored due to recent lower-than-average recruitment (Figure 32).

Future harvest levels were based on changes to the total allowable commercial catch (TACC). Four scenarios were run with the TACC increasing by 5% (94.5 t), 10% (99 t), 15% (103.5 t) and 20% (108 t). Future harvesting was assumed to have the same selectivity as the last year in the model.

The projected scenarios across all models were very similar and showed that under the most optimistic scenario (ten-year resampling and 5% TACC increase) the population would continue to increase. Under the most pessimistic situation with five-year resampling of recruitment and 20% TACC increase, the population will either stabilise or, in some situations, decrease slightly. Future recruitment assumptions had a slightly larger effect than those assumptions surrounding future harvest levels.

Under a 5% TACC increase the probability of the stock being above the target level of 40% B_0 for the base case increased from 93% in 2017 to 96% in 2020 (Figures 33–35). Future stock status (expressed as the probability of being above the target level of 40% B_0) for the year 2020 for other future scenarios and model runs are shown in Table 6. Model (0.6) was the only sensitivity run that had a small probability (less than 1%) that projected SSB would fall below the soft limit. Projected quantities across all models taken to MCMC are summarised in Tables 7–18.

4. DISCUSSION

The base case model suggested that the current spawning stock population ($B_{current}$) for 2017 was 47% (95% CI 38–61%) B_0 , and recruit-sized stock biomass ($B_{current}^r$) was 43% (95% CI 34–55%) of the initial recruit-sized state (B_t^r). The base case model suggested that the current stock status was very unlikely to fall below the target limit. The projections suggested that biomass was likely to remain constant if future catches were to be above the TACC by 5%. This was the similar conclusion across all sensitivity runs.

Overall, this assessment was quite robust to the assumptions explored during the process with most MPD runs suggesting a current relative biomass above the target (40%) of equilibrium size (B_0). This was anecdotally supported by some of the fishers who said that they thought the stock size was similar to that seen in the 1990s when the stock was last estimated to be at this level.

All the recent data sources in the assessment suggest that the stock has been improving since the mid-2000s with increasing CPUE and an increase in mean length, although the increase in mean length is a direct result of selective targeting i.e. increasing minimum harvest size. The combination of fishers targeting larger fish and maintaining high catch rates is indicative of a healthy stock.

This stock assessment had added benefits relative to previous paua stock assessments, in that natural mortality could be estimated with an uninformative prior. Natural mortality is an important component of uncertainty in other paua assessments, and is usually fixed with a highly informative prior. The ability to estimate natural mortality reduced the number of sensitivity runs required. There is still the limitation of having a time-invariant natural mortality over the period of interest, and this should be a model component that is investigated in the future.

The weaknesses of the assessment are similar to those of historic paua assessments where the main biomass observation is based on CPUE. Currently this analysis relies on Paua Catch Effort Landing Return (PCELR) forms which record daily fishing time and catch per diver on a relatively large spatial scale. These data are likely to remain the basis for stock assessments and formal management in the medium term. Since October 2010, a dive-logger data collection programme has been initiated to achieve fine-scale monitoring of paua fisheries (Neubauer & Abraham 2014, Neubauer et al. 2015). The use of the data loggers by paua divers and ACE holders has been steadily increasing over the last five years. Using fishing data logged at fine spatial and temporal scales could substantially improve effort calculations and associated CPUE indices, and allow complex metrics such as spatial CPUE to be developed (Neubauer 2015). Data from the loggers have been analysed to provide comprehensive descriptions of the spatial extent of the fisheries and insight on relationships between diver behaviour, CPUE, and changes in abundance on various spatial and temporal scales (Neubauer & Abraham 2014, Neubauer et al. 2015). However, the data-loggers can potentially change how the divers operate, such that they may become more effective in their fishing operations (the divers become capable of avoiding areas that have been heavily fished or that have relatively low CPUE), therefore changing the meaning of diver CPUE (Butterworth et al. 2015).

Future work for these assessments include investigating modelling at an appropriate spatial scale. The model treats the whole of the assessed area of PAU 5B as if it were a single stock with homogeneous

biology, habitat and fishing pressures. The model assumes homogeneity in recruitment and natural mortality, and that growth has the same mean and variance. However, it is known that localised variation and processes are important for paua (Breen et al. 1982, Laferriere 2015). For instance, if some local patches are fished very hard and others are not fished, recruitment failure can result because of the depletion of spawners. Spawners must breed close to each other and the dispersal of larvae is unknown and may be limited. Recruitment failure is a common observation in overseas abalone fisheries, suggesting that local processes may decrease recruitment, an effect that the current model cannot account for. The biology of paua adds a great deal of uncertainty into the model and future improvements could include a more spatially explicit model or simulations to understand the effects of ignoring such spatially variable processes.

Heterogeneity in growth can be a problem for length based models (Punt 2003). Variation in growth is addressed to some extent by having a stochastic growth transition matrix based on increments observed in multiple areas; similarly, the length frequency data are integrated across samples from many places. Relative weights were assigned, so that more productive areas in the fishery were better represented in the model. However, there is always a need for more data to help understand the variability of growth within a QMA.

5. ACKNOWLEDGMENTS

This work was supported by a contract from the Ministry for Primary Industries (PAU201701 Objective 1). Thank you to Paul Breen for developing the stock assessment model that was used in this assessment and for the use of major proportions of the 2006 report for this update. Thank you to the Shellfish Working Group for all the advice provided throughout the assessment process. Thank you to Ian Tuck, Adele Dutilloy, Kath Large and Matt Dunn for reviewing the draft report.

6. REFERENCES

- Andrew, N.L.; Breen, P.A.; Naylor, J.R.; Kendrick, T.H.; Gerring, P. (2000). Stock assessment of paua (*Haliotis iris*) in PAU 7 in 1998–99. *New Zealand Fisheries Assessment Report 2000/49*. 40 p.
- Breen, P.A.; Adkins, B.; Station, P.B. (1982). Observations of abalone populations on the north coast of British Columbia, July 1980. Department of Fisheries and Oceans, Resource Services Branch, Pacific Biological Station.
- Breen, P.A.; Andrew, N.L.; Kendrick, T.H. (2000a). Stock assessment of paua (*Haliotis iris*) in PAU 5B and PAU 5D using a new length-based model. *New Zealand Fisheries Assessment Report 2000/33*. 37 p.
- Breen, P.A.; Andrew, N.L.; Kendrick, T.H. (2000b). The 2000 stock assessment of paua (*Haliotis iris*) in PAU 5B using an improved Bayesian length-based model. *New Zealand Fisheries Assessment Report 2000/48*. 36 p.
- Breen, P.A.; Andrew, N.L.; Kim, S.W. (2001). The 2001 stock assessment of paua (*Haliotis iris*) in PAU 7. *New Zealand Fisheries Assessment Report 2001/55*. 53 p.
- Breen, P.A.; Kim, S.W. (2003). The 2003 stock assessment of paua (*Haliotis iris*) in PAU 7. *New Zealand Fisheries Assessment Report 2003/35*. 112 p.
- Breen, P.A.; Kim, S.W. (2004a). The 2004 stock assessment of paua (*Haliotis iris*) in PAU 4. *New Zealand Fisheries Assessment Report 2004/55*. 79 p.
- Breen, P.A.; Kim, S.W. (2004b). The 2004 stock assessment of paua (*Haliotis iris*) in PAU 5A. *New Zealand Fisheries Assessment Report 2004/40*. 86 p.
- Breen, P.A.; Kim, S.W. (2005). The 2005 stock assessment of paua (*Haliotis iris*) in PAU 7. *New Zealand Fisheries Assessment Report 2005/47*. 114 p.
- Breen, P.A.; Kim, S.W. (2007). The 2006 stock assessment of paua (*Haliotis iris*) stocks PAU 5A (Fiordland) and PAU 5D (Otago). *New Zealand Fisheries Assessment Report 2007/09*. 164 p.

- Breen, P.A.; Kim, S.W.; Andrew, N.L. (2003). A length-based Bayesian stock assessment model for abalone. *Marine and Freshwater Research* 54(5): 619–634.
- Breen, P.A.; Smith, A.N.H. (2008a). The 2007 assessment for paua (*Haliotis iris*) stock PAU 5B (Stewart Island). *New Zealand Fisheries Assessment Report 2008/05*.
- Breen, P.A.; Smith, A.N.H. (2008b). Data used in the 2007 assessment for paua (*Haliotis iris*) stock PAU 5B (Stewart Island). *New Zealand Fisheries Assessment Report 2008/6*. 45 p.
- Butterworth, D.; Haddon, M.; Haist, V.; Helidoniotis, F. (2015). Report on the New Zealand Paua stock assessment model; 2015. *New Zealand Fisheries Science Review* 2015/4. 31 p
- Cordue, P.L. (2009). Analysis of PAU5A dive survey data and PCELR catch and effort data. Final report for SeaFIC and PauaMAC5. (Unpublished report held by SeaFIC.)
- Francis, R.I.C.C. (2011). Data weighting in statistical fisheries stock assessment models. *Canadian Journal of Fisheries and Aquatic Sciences* 68: 1124–1138.
- Fu, D.; McKenzie, A. (2010a). The 2010 stock assessment of paua (*Haliotis iris*) for Chalky and South Coast in PAU 5A. *New Zealand Fisheries Assessment Report 2010/36*. 63 p.
- Fu, D.; McKenzie, A. (2010b). The 2010 stock assessment of paua (*Haliotis iris*) for Milford, George, Central, and Dusky in PAU 5A. *New Zealand Fisheries Assessment Report 2010/46*. 55 p.
- Fu, D. (2014a). The 2013 stock assessment of paua (*Haliotis iris*) for PAU 5B. *New Zealand Fisheries Assessment Report 2014/ 45*.
- Fu, D.; McKenzie, A; Naylor, R. (2014a). Summary of input data for the 2013 PAU 5B stock assessment. *New Zealand Fisheries Assessment Report 2014/43*. 61 p.
- Haist, V. (2010). Paua research diver survey: review of data collected and simulation study of survey method. *New Zealand Fisheries Assessment Report 2010/38*. 54 p.
- Kim, S.W.; Bentley, N.; Starr, P.J.; Breen, P.A. (2004). Assessment of red rock lobsters (*Jasus edwardsii*) in CRA 4 and CRA 5 in 2003. *New Zealand Fisheries Assessment Report 2004/8*. 165 p.
- Laferriere, M.A. (2015) Examining the ecological complexities of blackfoot paua demography and habitat requirements in the scope of marine reserve protection (Doctoral dissertation). Available from <http://researcharchive.vuw.ac.nz/xmlui/bitstream/handle/10063/5189/thesis.pdf?sequence=1>.
- Marsh, C.; Fu, D. (2017) The 2016 stock assessment of paua (*Haliotis iris*) in PAU 5D. *New Zealand Fisheries Assessment Report 2017/33*.
- Marsh, C.; McKenzie, A; Naylor, R. (2018). Summary of input data for the 2017 PAU 5B stock assessment. *New Zealand Fisheries Assessment Report 2018/22*.
- McKenzie, A.; Smith, A.N.H. (2009a). The 2008 stock assessment of paua (*Haliotis iris*) in PAU 7. *New Zealand Fisheries Assessment Report 2009/34*. 84 p.
- McKenzie, A.; Smith, A.N.H. (2009b). Data inputs for the PAU 7 stock assessment in 2008. *New Zealand Fisheries Assessment Report 2009/33*. 34 p.
- McShane, P.E.; Mercer, S.F.; Naylor, J.R. (1994). Spatial variation and commercial fishing of the New Zealand paua (*Haliotis iris* and *H. australis*). *New Zealand Journal of Marine and Freshwater Research* 28: 345–355.
- McShane, P.E.; Mercer, S.; Naylor, J.R.; Notman, P.R. (1996). Paua (*Haliotis iris*) fishery assessment in PAU 5, 6, and 7. New Zealand Fisheries Assessment Research Document 96/11. 35 p. (Unpublished report held in NIWA library, Wellington.)
- Neubauer, P. (2015). Alternative CPUE indices for PAU7, 11 p. Unpublished report prepared for the Shellfish Working Group.
- Neubauer, P.; Abraham, E. (2014). Using GPS logger data to monitor change in the PAU 7 pāua (*Haliotis iris*) fishery. *New Zealand Fisheries Assessment Report 2014/31*. 18 p.
- Neubauer, P.; Abraham, E.; Know, C.; Richard, Yvan. R. (2015). Assessing the performance of paua (*Haliotis iris*) fisheries using GPS logger data. *New Zealand Fisheries Assessment Report 2015/71*.
- Punt, A.E. (2003). The performance of a size-structured stock assessment method in the face of spatial heterogeneity in growth. *Fisheries Research* 65: 391–409.
- Schiel, D.R. (1989). Paua fishery assessment 1989. New Zealand Fisheries Assessment Research Document 89/9: 20 p. (Unpublished report held in NIWA library, Wellington, New Zealand.)

- Schiel, D.R. (1992). The paua (abalone) fishery of New Zealand. *In: Abalone of the world: Biology, fisheries and culture*. Shepherd, S.A.; Tegner, M.J.; Guzman del Proo, S. (eds.) pp. 427–437. Blackwell Scientific, Oxford.
- Scheil, D.R.; Breen, P.A. (1991). Population structure, aging, and fishing mortality of the New Zealand abalone *H. iris*. *Fishery Bulletin*, 89: 681–691.
- Schnute, J. (1985). A General Theory for Analysis of Catch and Effort Data. *Canadian Journal of Fisheries and Aquatic Sciences* 42(3): 414–429.
- Shepherd, S.A.; Rodda, K.R.; Vargas, K.M. (2001). A chronicle of collapse in two abalone stocks with proposals for precautionary management. *Journal of Shellfish Research* 20: 843–856.
- Thorson, J.T.; Cope, J.M. (2017). Uniform, uninformed or misinformed?: The lingering challenge of minimally informative priors in data-limited Bayesian stock assessments. *Journal of Fisheries Research* 194: 164–172.

Table 1: Actual sample sizes, initial sample sizes determined for the multinomial likelihood, and model weighted sample sizes for the PAU 5B commercial catch sampling length frequencies from the base model (0.1). A description of the model runs is summarised in Table 5.

Fishing year	Actual sample size	Initial sample size	Final model sample size
1992	18 815	3230	73
1993	15500	2064	46
1994	13390	2133	48
1998	1054	257	6
1999	4541	1182	27
2000	2810	625	14
2001	2707	789	18
2002	3769	722	16
2003	3588	1114	25
2004	6123	1484	33
2005	3002	733	16
2006	2632	1120	25
2007	3537	1180	27
2008	4184	945	21
2009	5016	1547	35
2010	6855	1381	31
2011	5829	805	18
2012	5472	969	22
2013	7316	1063	24
2014	8890	1417	32
2015	7094	2024	46
2016	6848	1713	39
2017	6925	NA	NA

Table 2: Base case model specifications: for estimated parameters, the phase of estimation, type of prior, (U, uniform; N, normal; LN, lognormal), mean and CV of the prior, lower bound and upper bound.

Parameter	Phase	Prior	μ	CV	Lower	Upper
$\ln(R_0)$	1	U	–	–	5	50
M	3	U	–	–	0.01	0.5
g_1	2	U	–	–	0.01	150
g_2	2	U	–	–	0.01	150
g_{50}	2	U	–	–	0.01	150
$g_{50-95\%}$	2	U	–	–	0.01	150
g_{max}	1	U	–	–	0.01	50
α	2	U	–	–	0.01	10
β	2	U	–	–	0.01	10
$\ln(q^I)$	1	U	–	–	-30	0
$\ln(q^J)$	1	U	–	–	-30	0
L_{50}	1	U	–	–	70	145
L_{95-50}	1	U	–	–	1	50
D_{50}	2	U	–	–	70	145
D_{95-50}	2	U	–	–	0.01	50
D_s	1	U	–	–	0.01	10
ε	1	N	0	0.4	-2.3	2.3

Table 3: Values for fixed quantities for base case model.

Variable	Value
L1	75
L2	120
a	2.99E-08
b	3.303
U^{max}	0.80
σ_{min}	1
σ_{obs}	0.25
$\tilde{\sigma}$	0.2
h	0.75

Table 4: Summary descriptions of base case (0.1) and sensitivity model runs.

Model	Description
0.1	inverse logistic growth model, tag-recapture weighted, CSLF data up to 2016, M prior Uniform, tag data > 70mm, RDLF and RDSI included, Combined CPUE series, Catch history assumption 3
0.1 all	The same as model 0.1 with CSLF data up to and including the 2017 fishing year.
0.2	Model 0.1 with split CPUE series, one for the CELR and another for the PCELR
0.3	Model 0.1 but with the RDLF and RDSI data excluded
0.4	Model 0.1 but with catch history assumption 1
0.5	Model 0.1 but start modelling at 2 mm instead of 70 mm
0.6	Model 0.1 but with a time varying catchability coefficient, with an estimated drift parameter ~ Uniform(-0.05, 0.05)

Table 5: MPD estimates for base case and sensitivity trials. “–” indicates that parameter is fixed and likelihood contributions were not used when datasets were removed. SDNRs for CSLF were calculated from mean length.

	0.1	0.1 all cslf	0.2	0.3	0.4	0.5	0.6
Parameters							
$\ln(R_0)$	13.81	13.82	13.79	13.83	13.91	13.95	13.71
M	0.10	0.10	0.09	0.10	0.09	0.10	0.09
L_{50}	95.25	95.25	95.26	95.25	95.26	95.24	95.25
L_{95-50}	18.86	18.86	18.88	18.86	18.91	18.89	18.89
D_{50}	125.37	125.37	125.28	125.53	125.22	125.38	125.38
D_{95-50}	3.03	3.06	3.02	3.24	2.91	3.04	3.05
D^s	0.82	0.84	0.84	0.81	0.84	0.82	0.82
T_{50}	102.87	104.03	101.81	112.30	101.20	102.97	101.96
T_{95-50}	26.96	26.17	25.10	33.70	24.17	25.58	25.82
q^l	-13.67	-13.65	-13.70	-13.68	-13.82	-13.67	-13.69
q^{l2}	-	-	-13.80	-	-	-	-
q^{RDSI}	-15.11	-15.09	-15.16	-	-15.24	-15.12	-15.06
l_{50}^g	78.04	84.21	80.58	83.87	80.72	77.62	79.90
l_{95-50}^g	66.27	62.35	63.87	61.56	63.74	66.28	64.77
Δ_{max}	49.00	42.60	46.34	43.03	46.20	49.75	47.01
α	0.72	1.43	0.73	0.75	0.73	0.74	0.73
β	0.72	0.45	0.71	0.69	0.71	0.70	0.71
q_{drift}^l	-	-	-	-	-	-	0.01
Indicators							
B_0	3869	3839	3924	3879	4404	3870	3863
$B_{current}$	1776	1782	1781	1816	2062	1780	1539
$B_{current}/B_0$	0.46	0.46	0.45	0.47	0.47	0.46	0.40
B_0^r	3475	3440	3530	3475	3964	3474	3499
$B_{current}^r$	1431	1434	1436	1461	1675	1436	1227
$B_{current}^r/B_0^r$	0.41	0.42	0.41	0.42	0.42	0.41	0.35
$U_{current}$	0.09	0.09	0.09	0.09	0.08	0.09	0.11
SDNR							
CPUE	0.92	0.94	0.66	0.93	0.92	0.93	0.93
CPUE2	0.00	0.00	0.92	0.00	0.00	0.00	0.00
RDSI	1.60	1.59	1.59	1.63	1.53	1.61	1.54
CSLF	1.00	1.00	0.98	1.00	1.00	1.00	0.99
RDLF	0.29	0.30	0.27	1.53	0.31	0.28	0.26
tag	1.15	1.02	1.16	1.16	1.16	1.15	1.15
mat	0.26	0.26	0.26	0.26	0.26	0.26	0.26

Table 6: Current stock status, and future (2020) stock status under four future assumptions on exploitation and recruitment. Stock status defined as: current, $Pr(B_{2017} > 40\%B_0)$; future, $Pr(B_{proj} > 40\%B_0)$.

Recruitment resampling	Current stock status		Future stock status			
			5% TACC increase		20% TACC increase	
			Five-years	Ten-years	Five-years	Ten-years
Base model (0.1)		93%	88%	93%	85%	91%
0.4		95%	92%	96%	90%	94%
0.6		67%	67%	71%	63%	68%

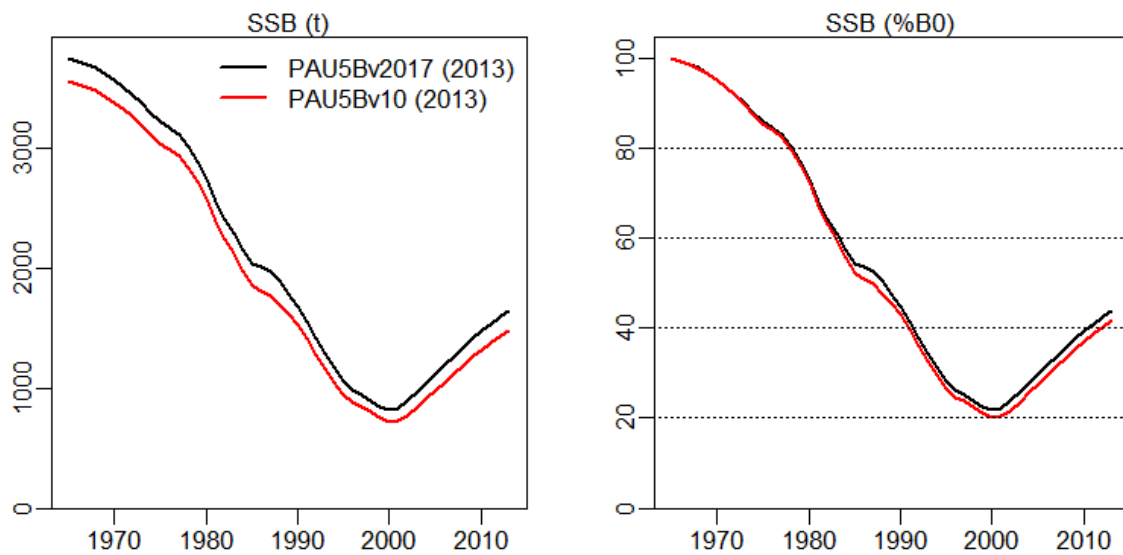


Figure 1: Comparison between the previous base model for this stock (PAU5Bv10 (2013)) and the updated model (PAU5Bv2017 (2013)).

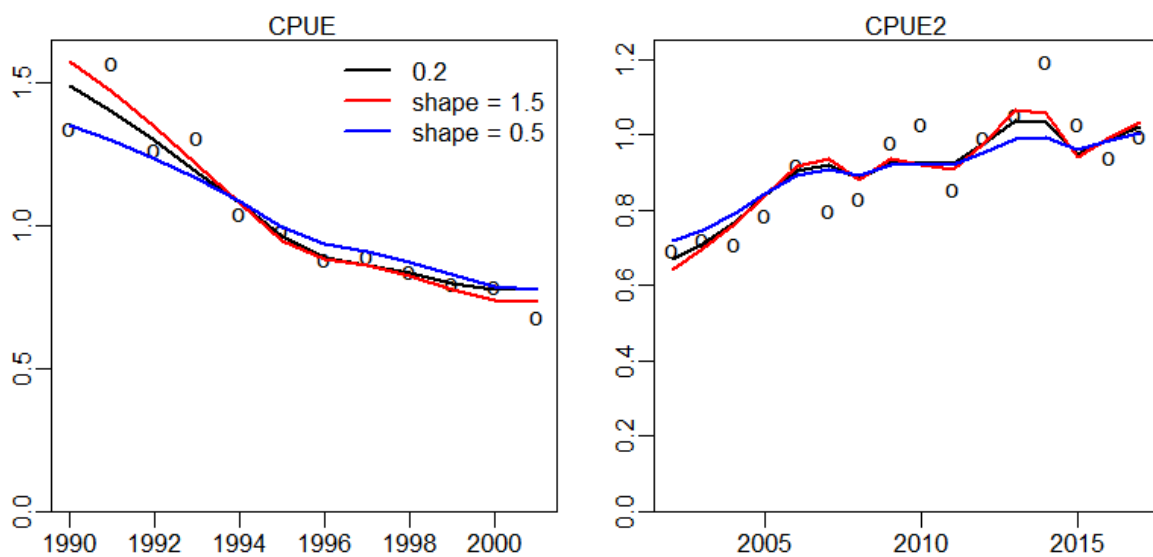


Figure 2: Comparing fits to CPUE series model runs with alternative values of the shape parameter (\tilde{b}). The black line (0.2) had a value of \tilde{b} .

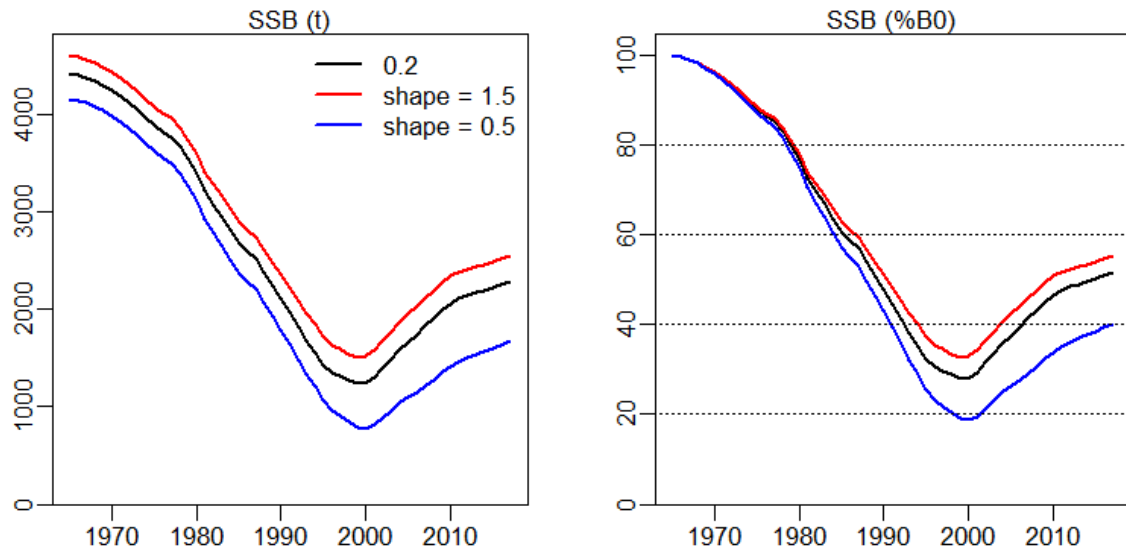


Figure 3: Comparing SSBs from model runs with alternative values of the shape parameter (\tilde{b}). The black line (0.2) had a value of $\tilde{b} = 0.2$.

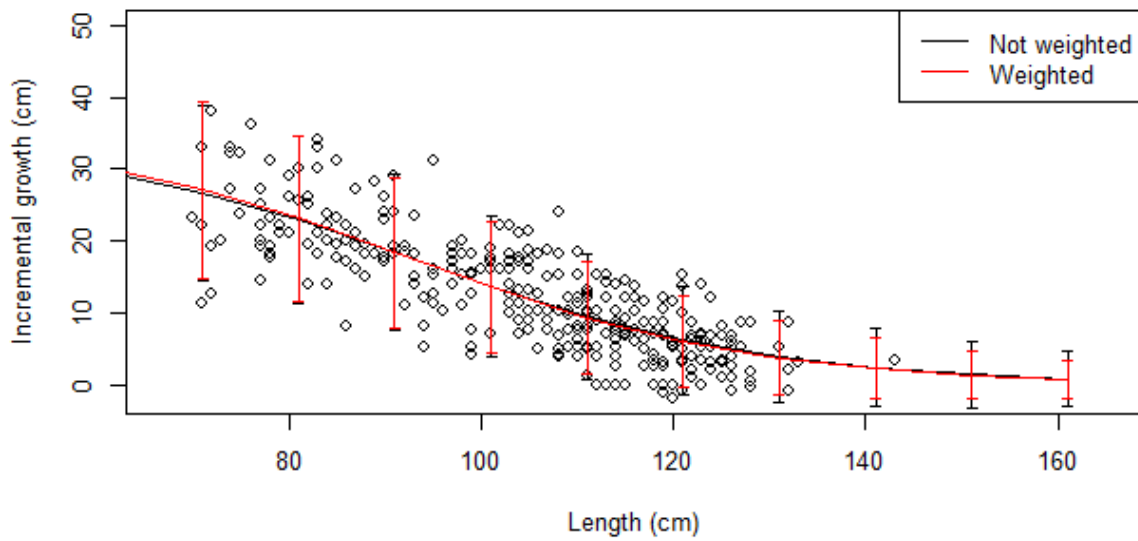


Figure 4: Comparison in growth fit, when weighting tag data by stratum.

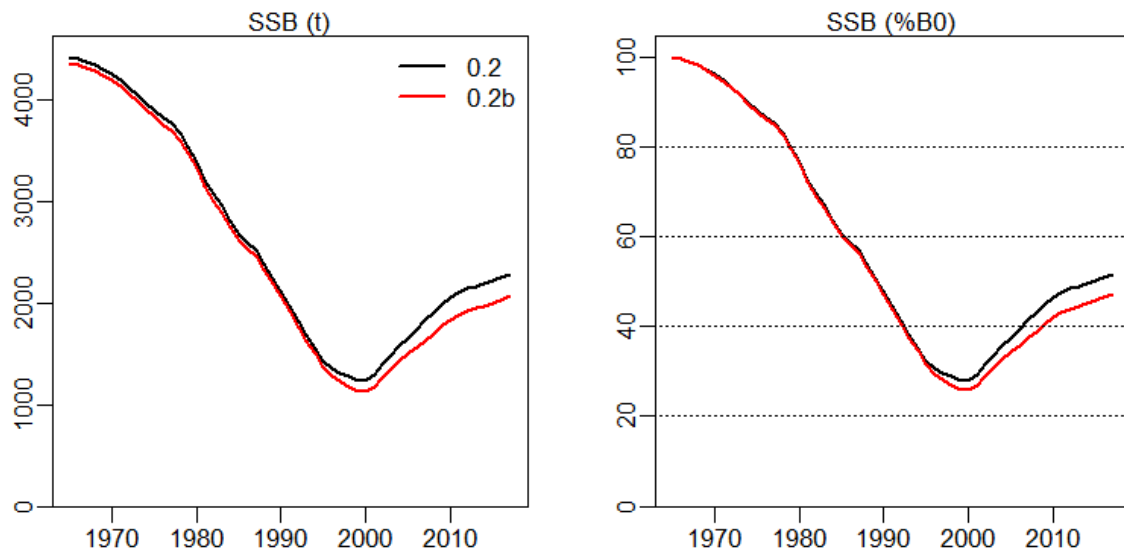


Figure 5: Comparison of SSBs between models that included RDLF and RDSI (0.2b) and a model run excluding it (0.2).

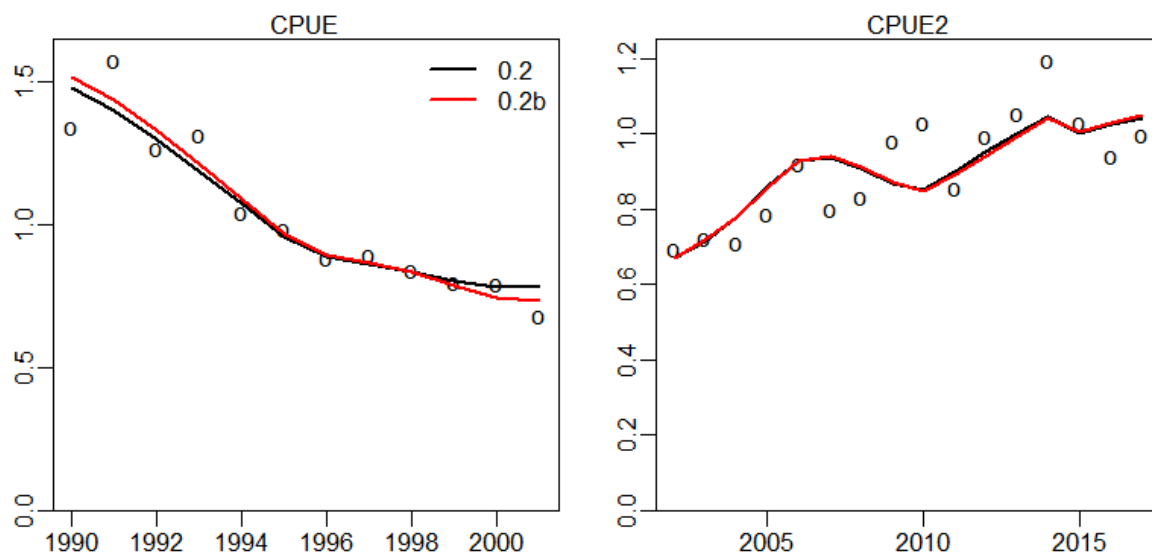


Figure 6: Model fits to CPUE datasets, model 0.2 excludes the research diver datasets and model 0.2b has the research diver information included.

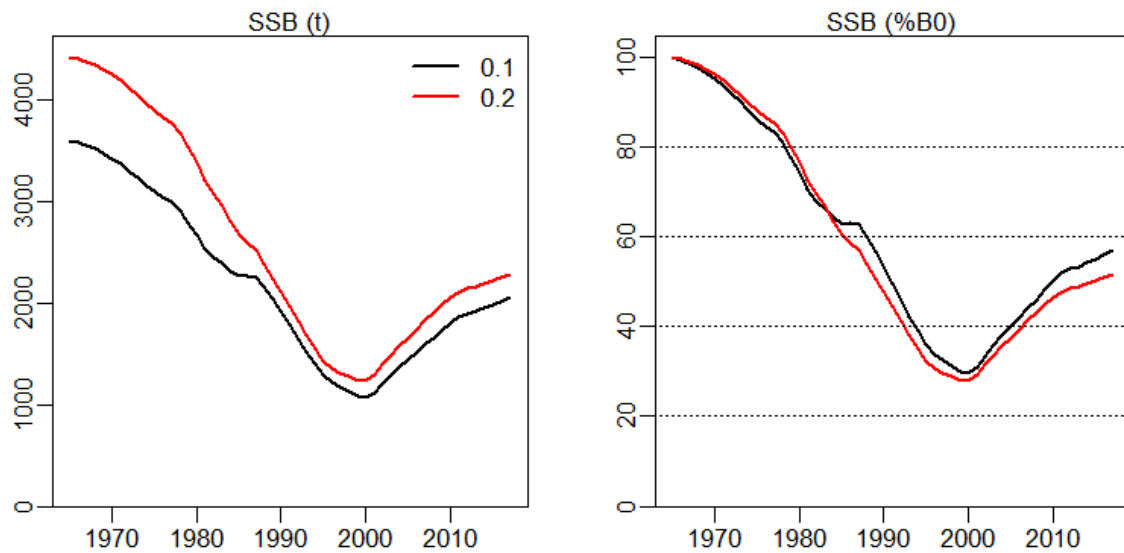


Figure 7: Comparing spawning stock biomass with different growth models, exponential (0.1) and inverse logistic (0.2).

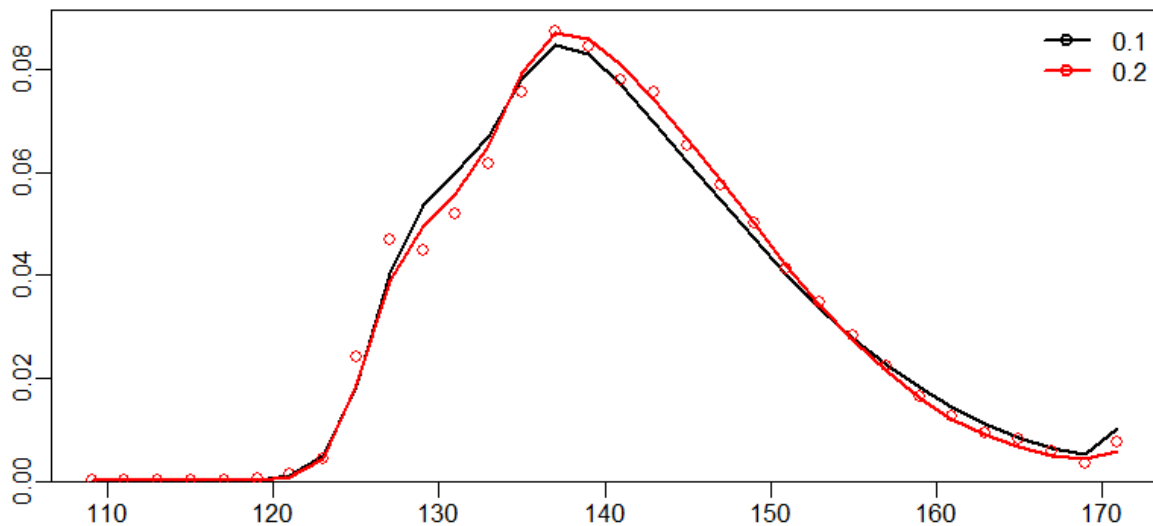


Figure 8: Fits to CSLF from models with different growth curves, the inverse logistic (0.2) and exponential (0.1).

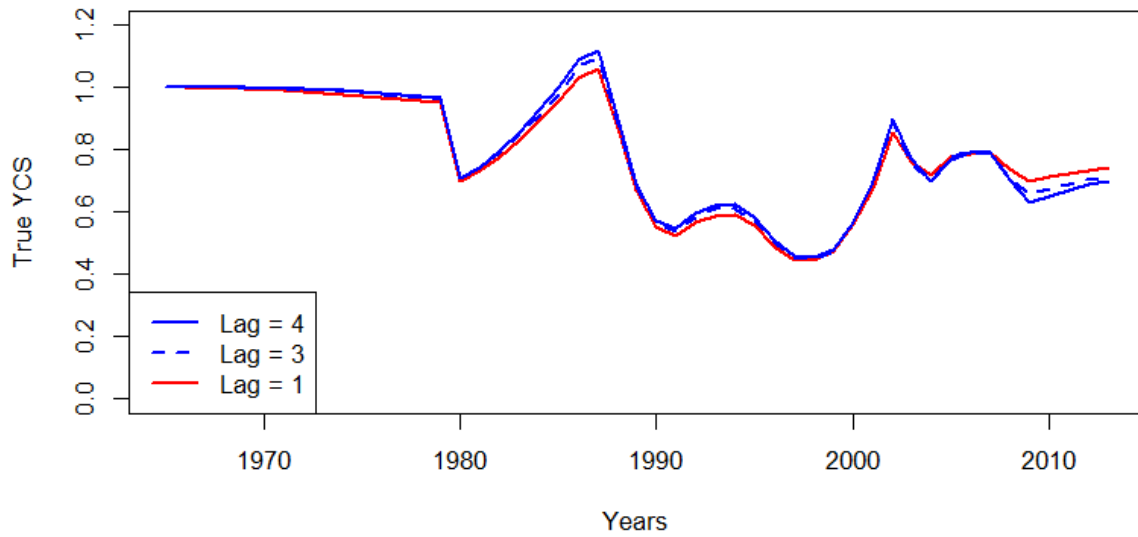


Figure 9: Comparison of true year class strength between models with different yearly lags between spawning and recruits entering the partition, for the recruitment dynamic.

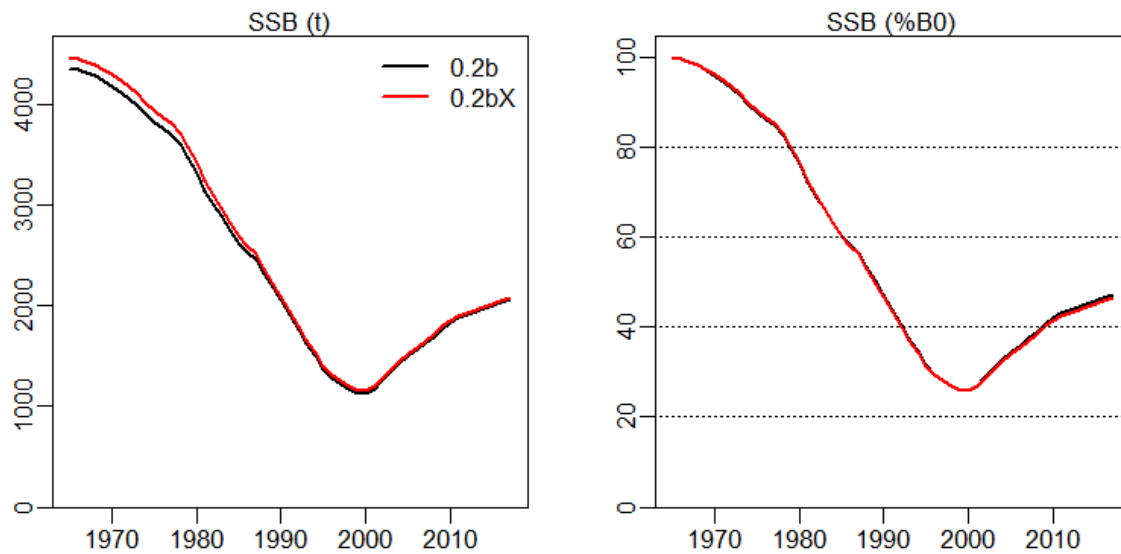


Figure 10: Comparison between starting the partition at 2 mm (0.2bX) compared with starting the partition at 70 mm (0.2b).

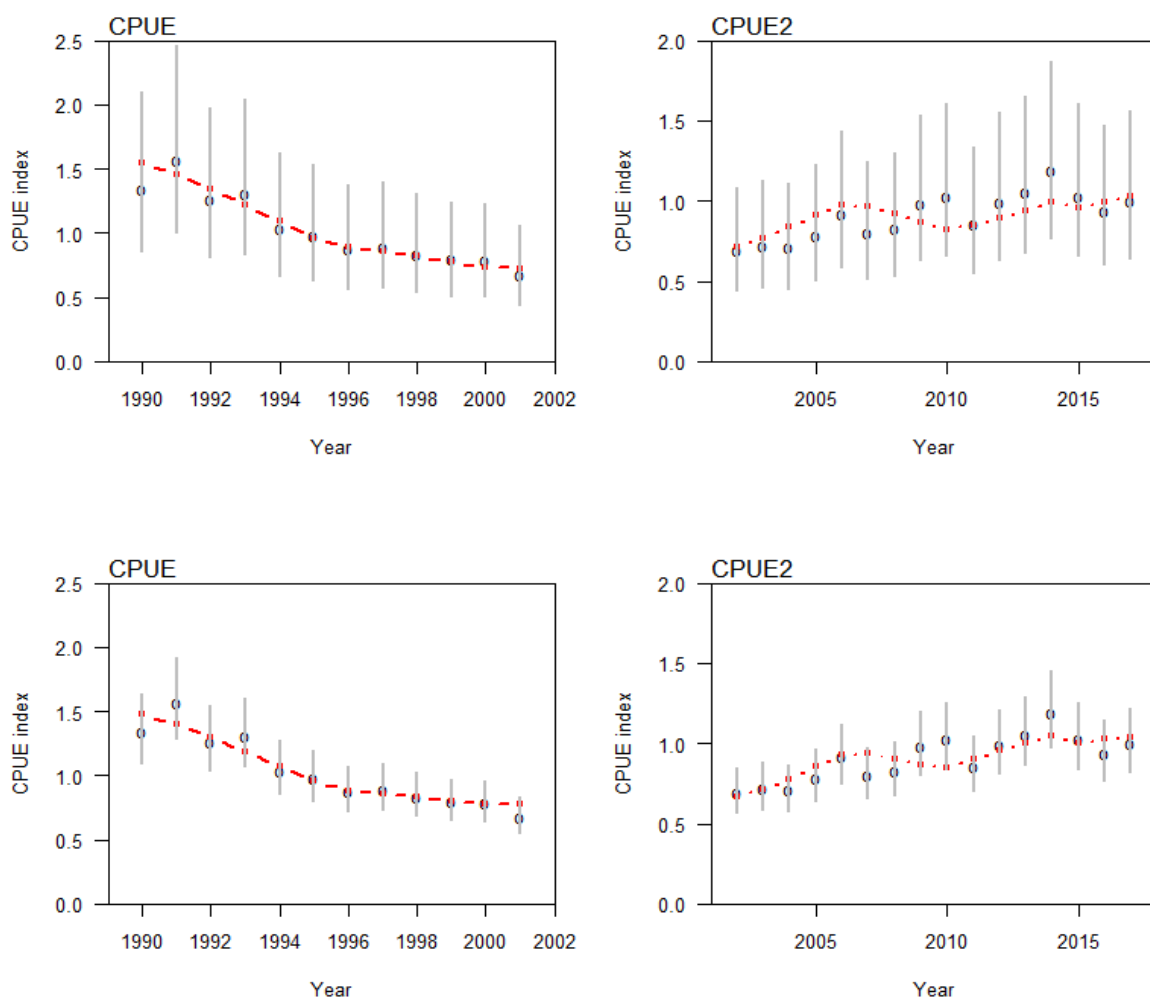


Figure 11: Fits to the two CPUE series, the top panels are from a model with additional error on the CPUE (20% additional process error). The bottom panels are with the base case value of 10% CV.

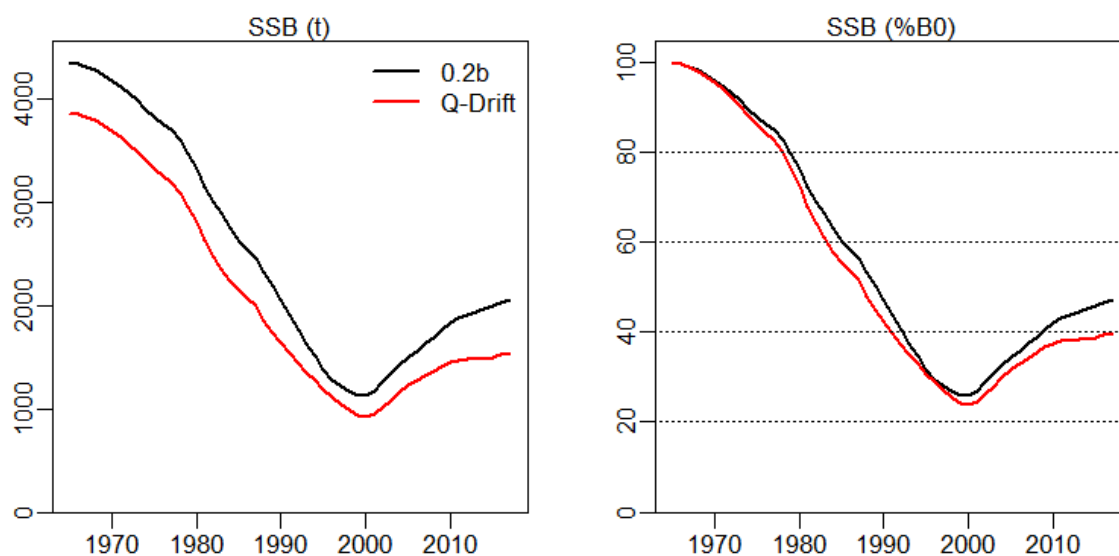


Figure 12: Comparison of SSBs showing the effect of allowing the catchability parameter to vary over the series.

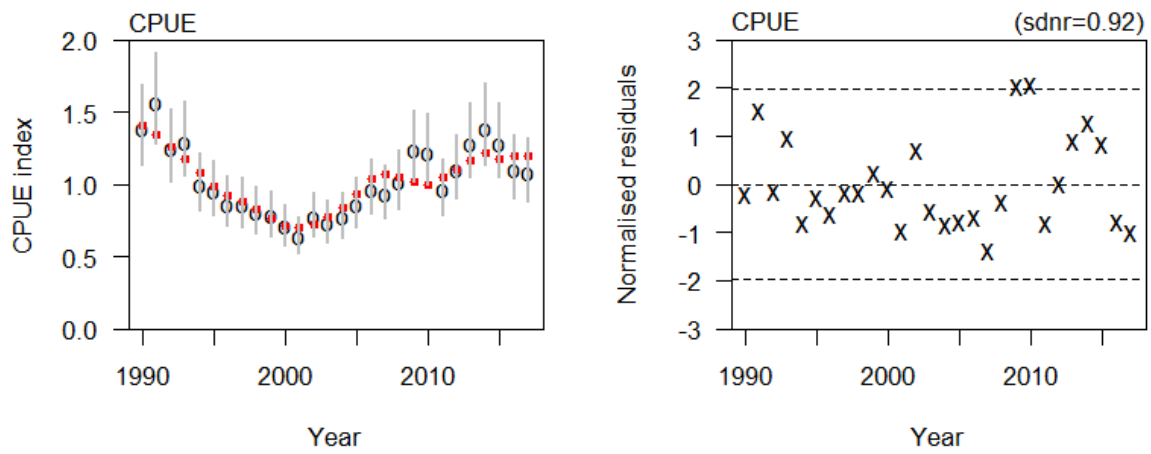


Figure 13: MPD fits to the CPUE series from the base case model.

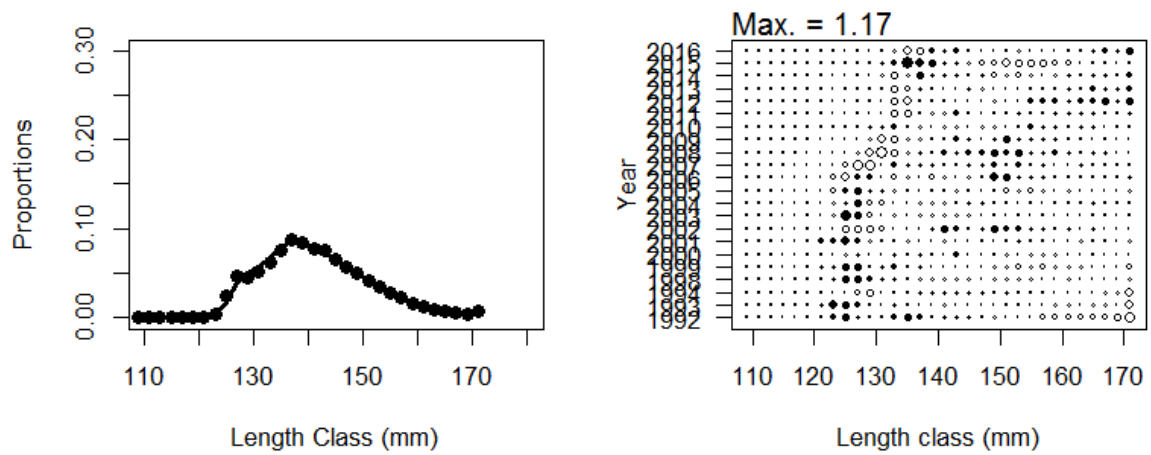


Figure 14: MPD fits to CSLF data for the base case model, left panel shows average fit to all years, right panel shows normalised residuals by year and length bin.

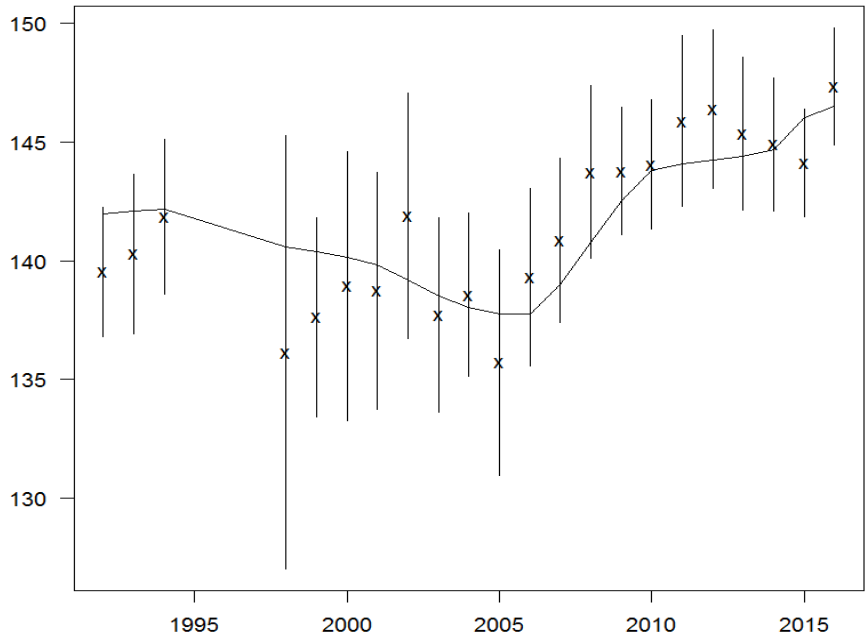


Figure 15: Mean length (cm y-axis) observed with standard errors (vertical bars) with the base model expectation as the fitted line, for available years (x-axis).

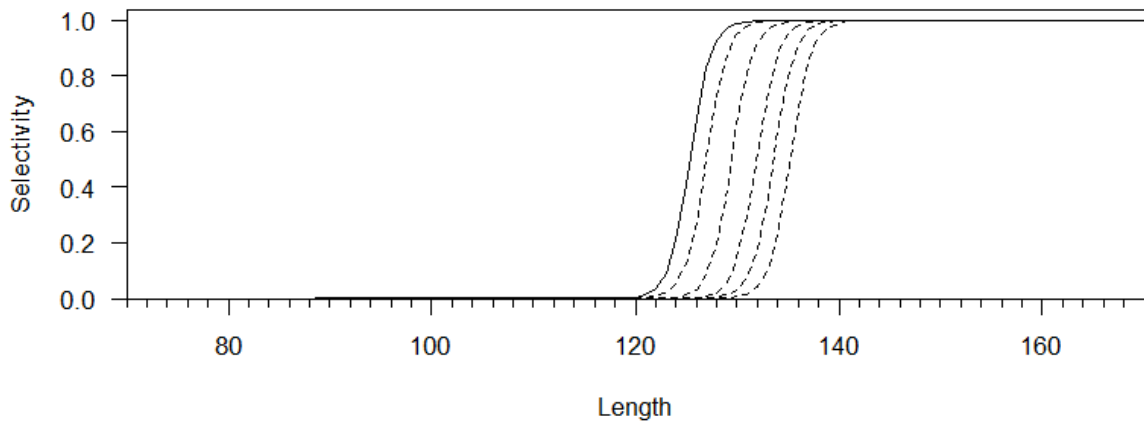


Figure 16: The selectivity ogive in the base case model.

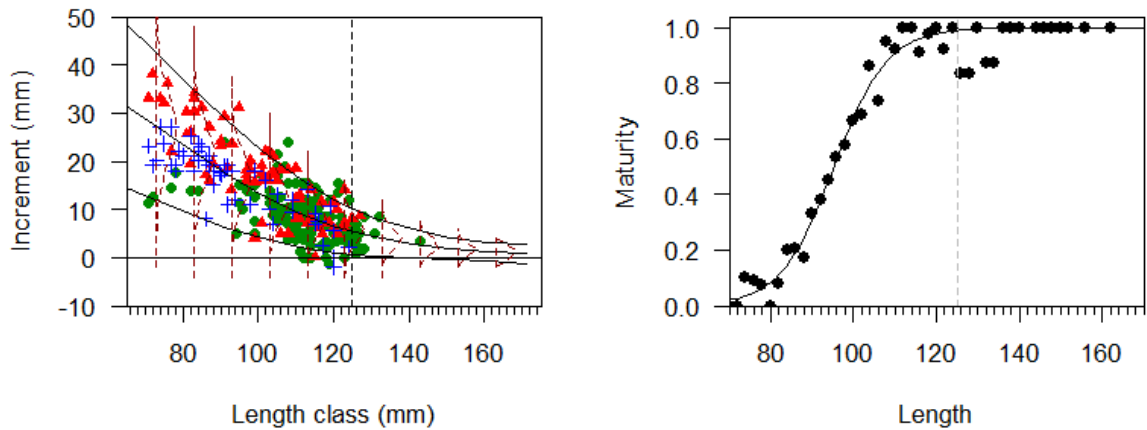


Figure 17: MPD fits to the tag recapture data (left panel) and maturity at length data (right panel) for the base case model.

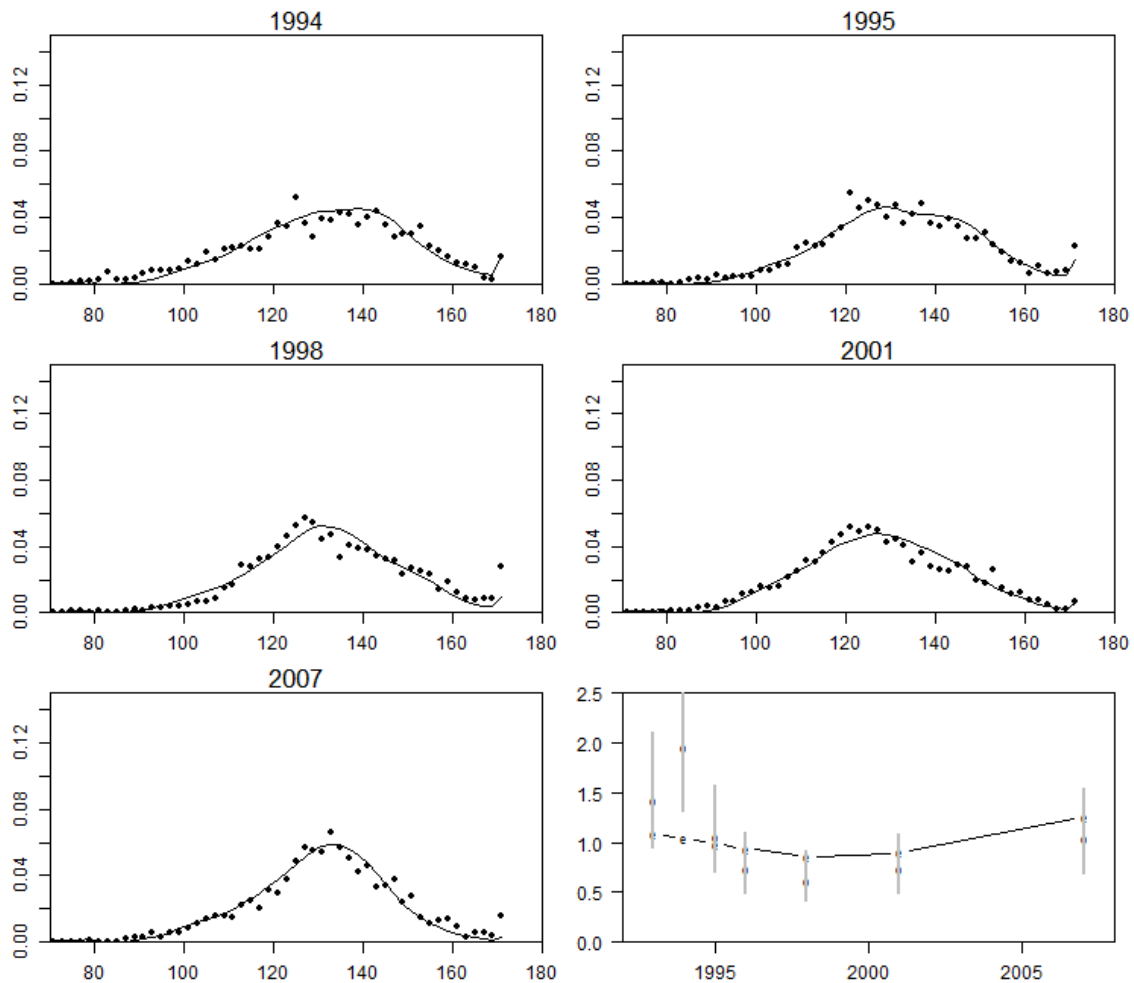


Figure 18: MPD fits for the base case model to the RDLF in first five panels, where dots are observed data and the line is the models expected fit of proportions (y-axis) for each length bin (x-axis), and the RDSI (bottom right panel), **where dot and vertical bars are observed relative abundance plus or minus two standard errors for each year available.**

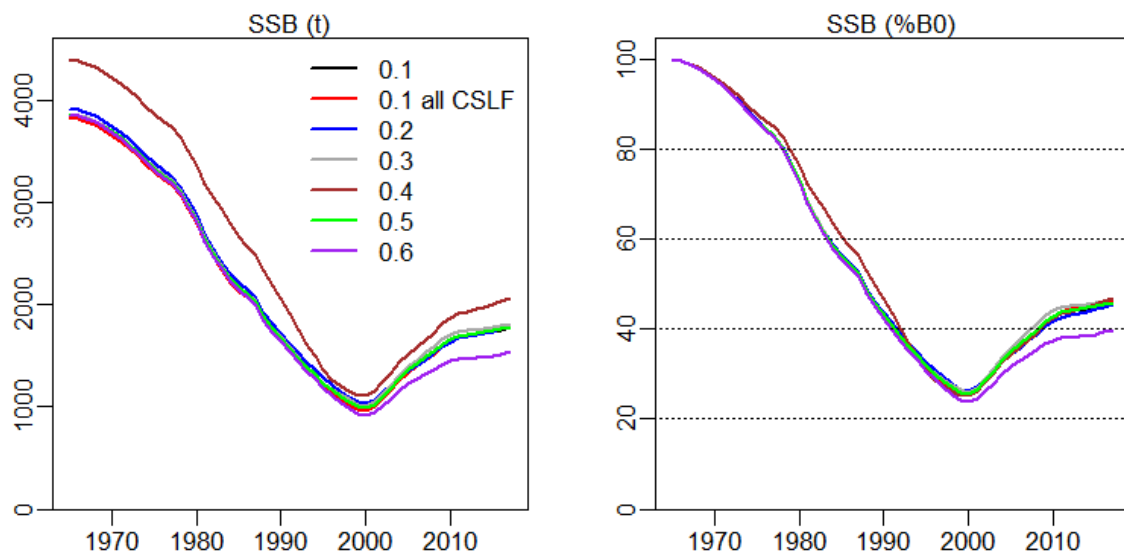


Figure 19: SSB trajectories for proposed base case model and sensitivity runs, from the initial ensemble of models.

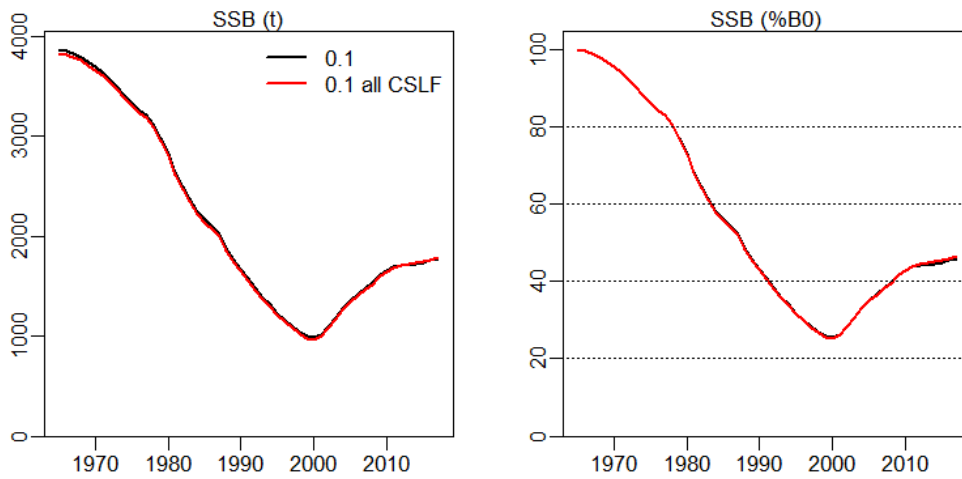


Figure 20: SSB trajectories comparing the base case model that included CSLF data up to the 2016 fishing year, and the same model with the additional 2017 CSLF data.

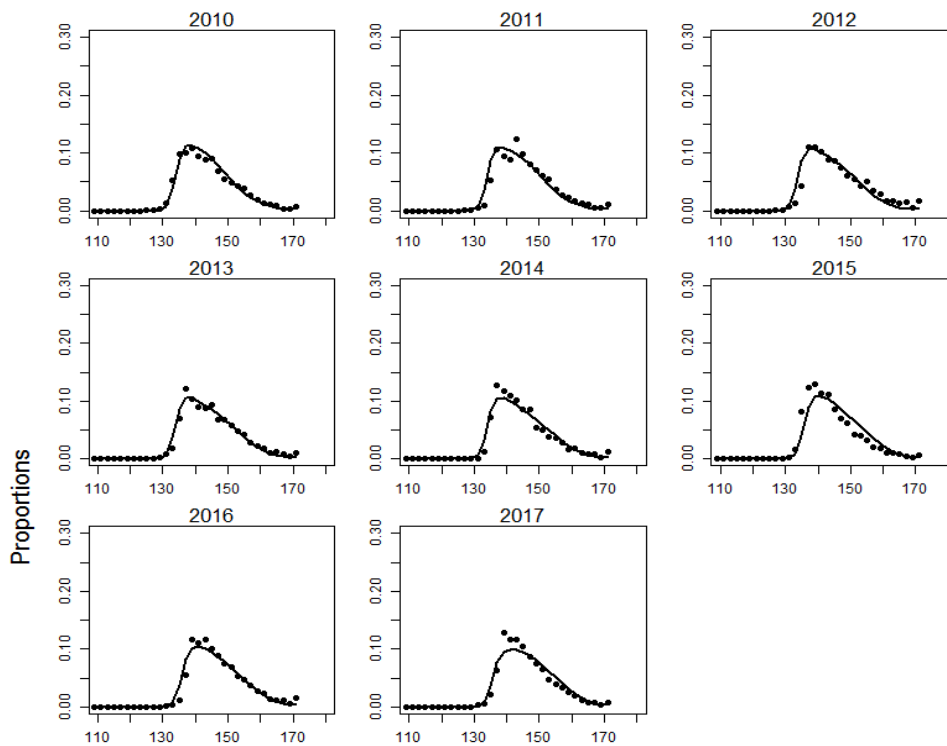


Figure 21: Fits to recent CSLF data from the base case model with the inclusion of the 2017 CSLF data.

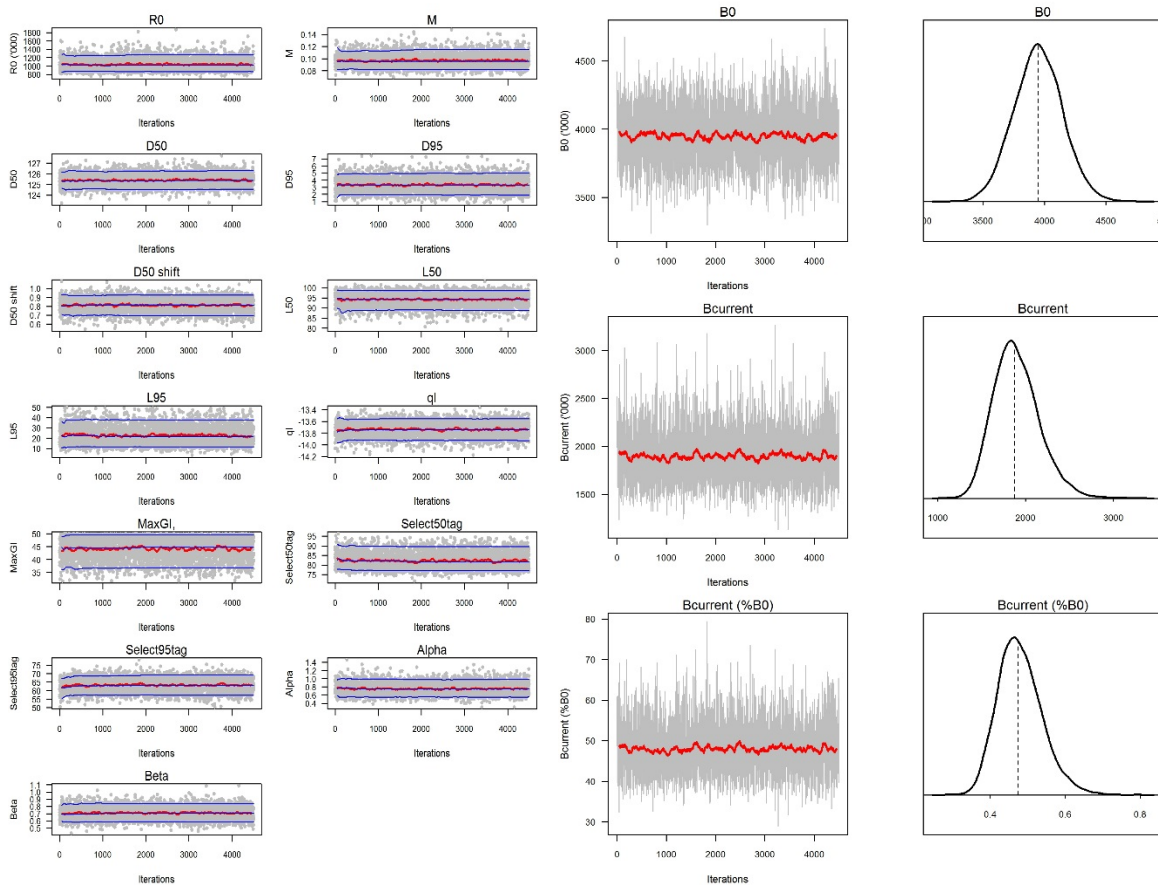


Figure 22: Trace plots and marginal posteriors for key productivity parameters and model quantities, for the base case model (0.1).

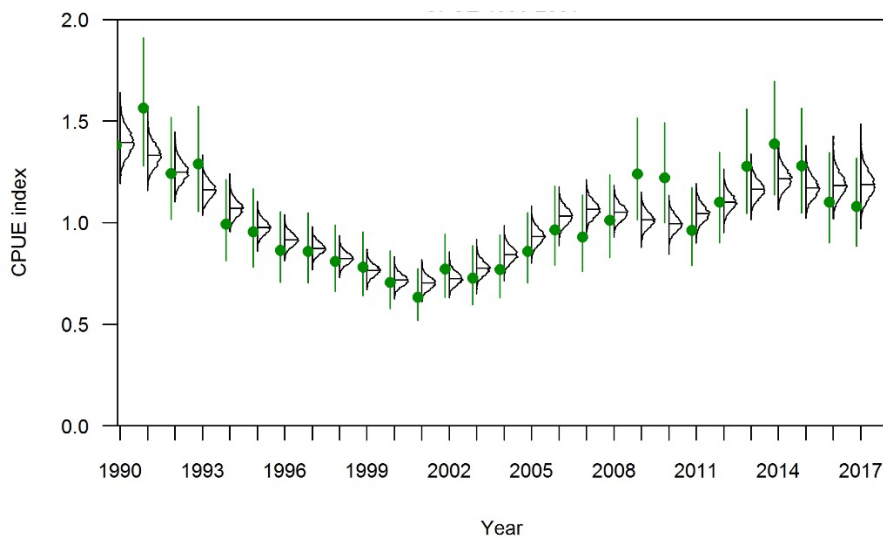


Figure 23: Predicted fits from the posterior compared to the observations (green) for the base case model.

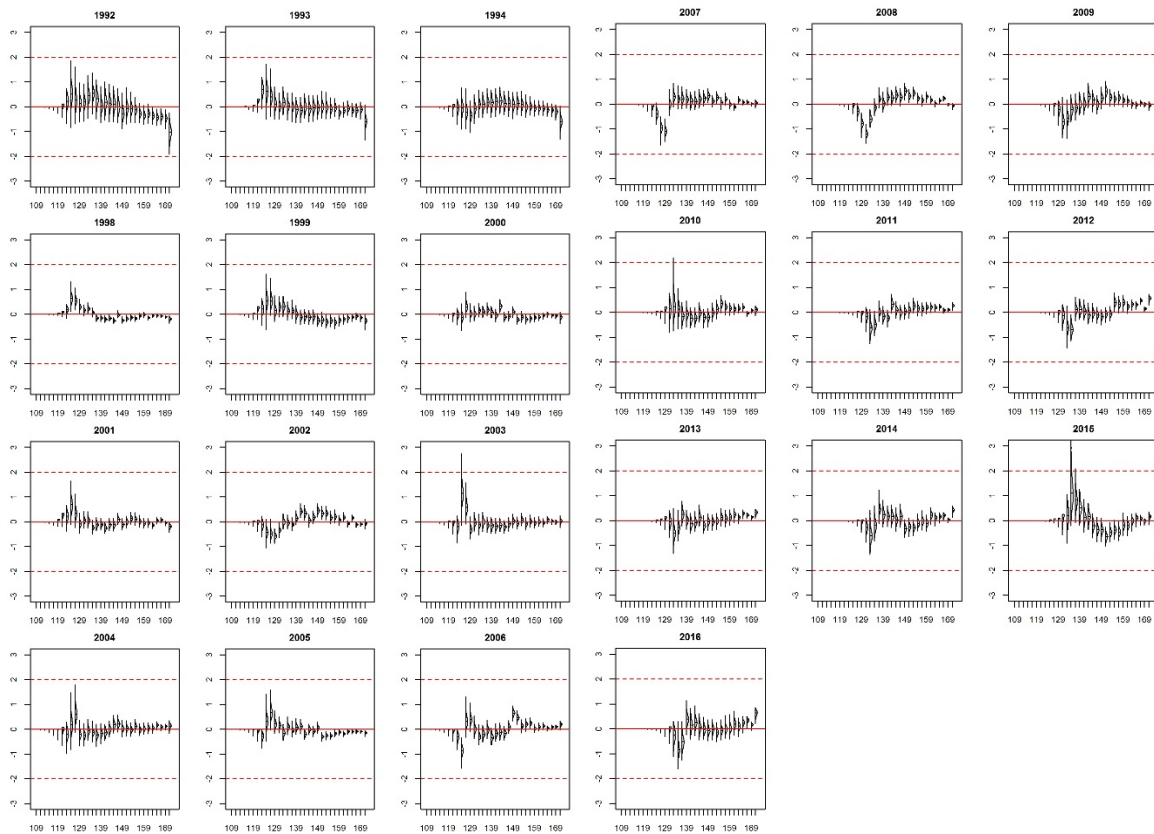


Figure 24: Standardised residuals for the CSLF observations, from the base case model.

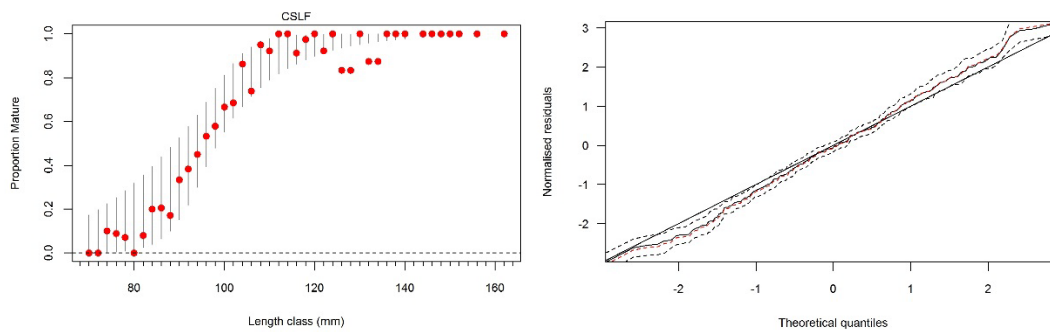


Figure 25: Left panel shows MCMC fits to length at maturity data, red dots are observations and vertical lines are 95% credible predictions. The right panel shows theoretical residuals vs observed residuals from the tag recapture observations, from the base case model.

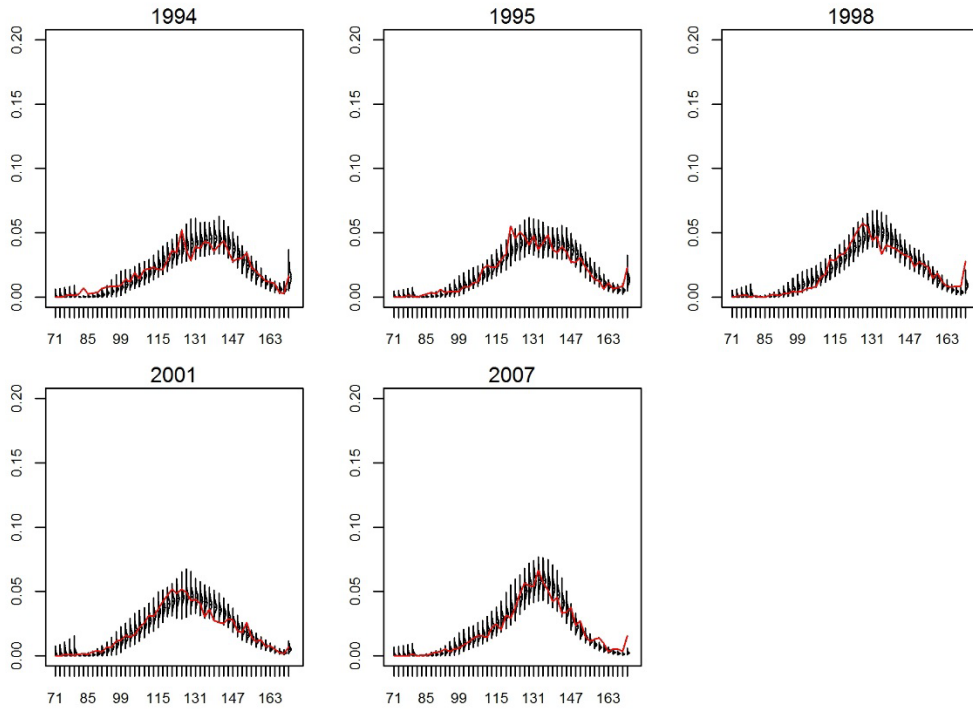


Figure 26: MCMC fits to RDLF data, red line is the observed length proportions the vertical density plots are the 95% credible predictions generated from the MCMC procedure, for the base case model.

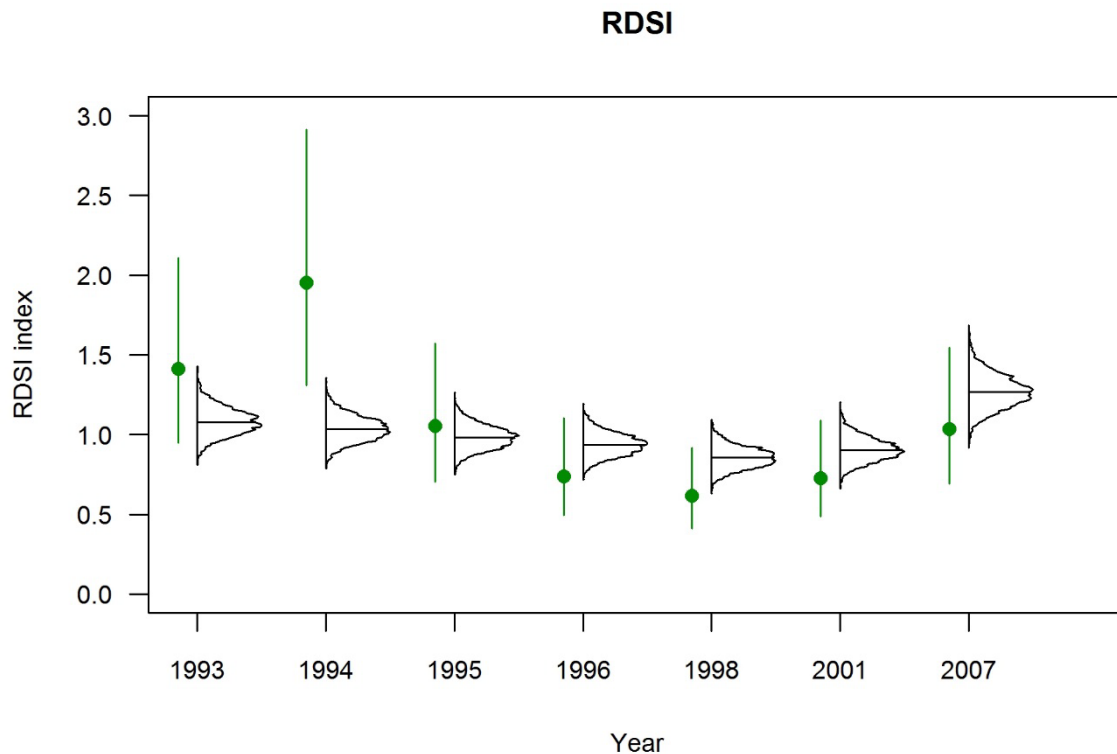


Figure 27: MCMC posterior predictions (densities) for RDSI data (green dot) plus or minus two standard errors (green bar), for the base case model.

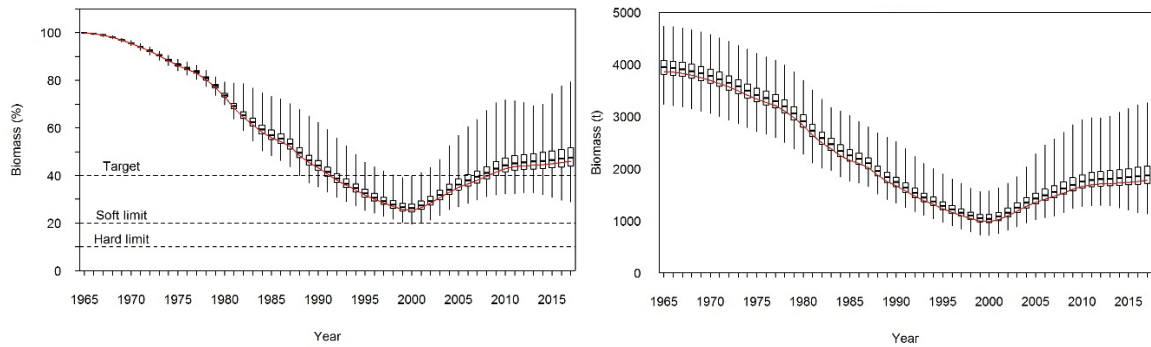


Figure 28: Left panel shows the SSB relative to an assumed equilibrium spawning biomass. Right panel is the absolute SSB over the model time interval. The red line shows SSB trajectory from the MPD fit.

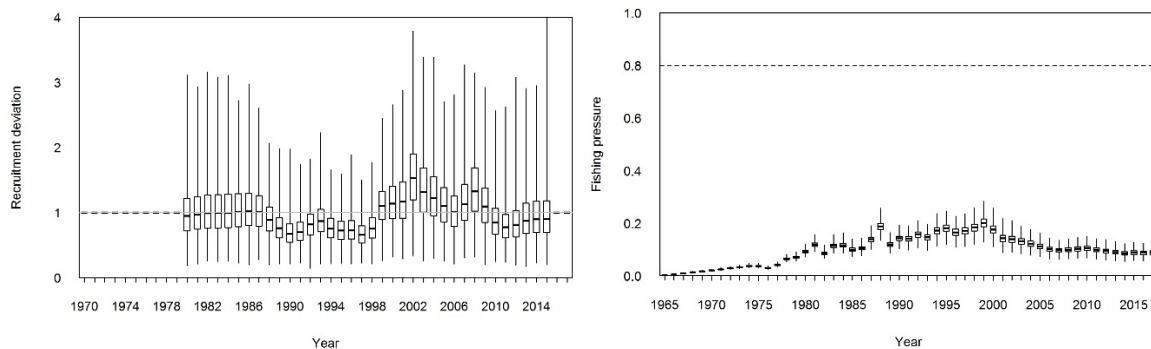


Figure 29: Marginal posteriors of model quantities, left panel estimated stock recruitment residuals (recruitment deviations). On the right panel exploitation rates derived from the base case model.

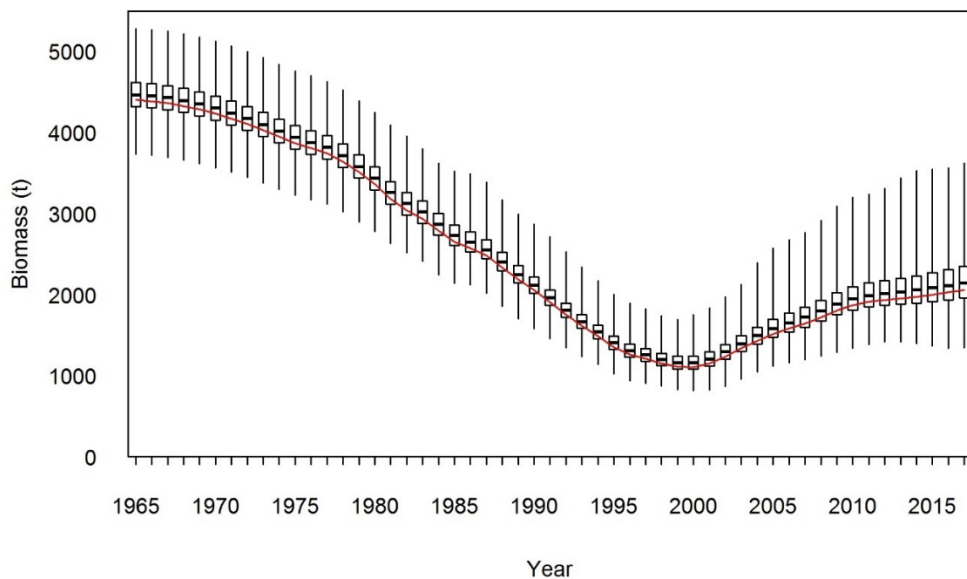


Figure 30: Box and whisker plot of absolute SSB from model run 0.4. The red line shows the SSB trajectory from the MPD fit.

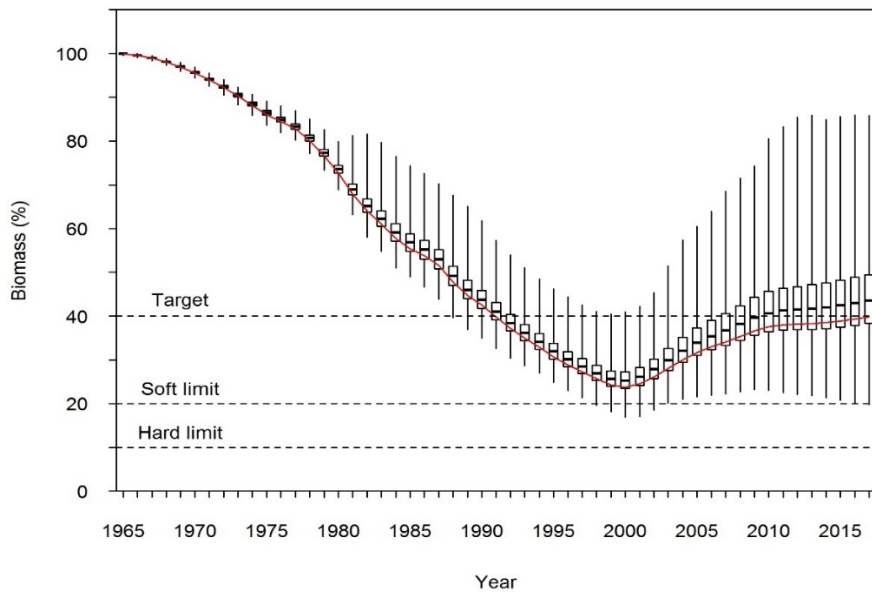


Figure 31: Box and whisker plots of relative SSB to an assumed equilibrium spawning biomass by year. The red line shows SSB trajectory from the MPD fit.

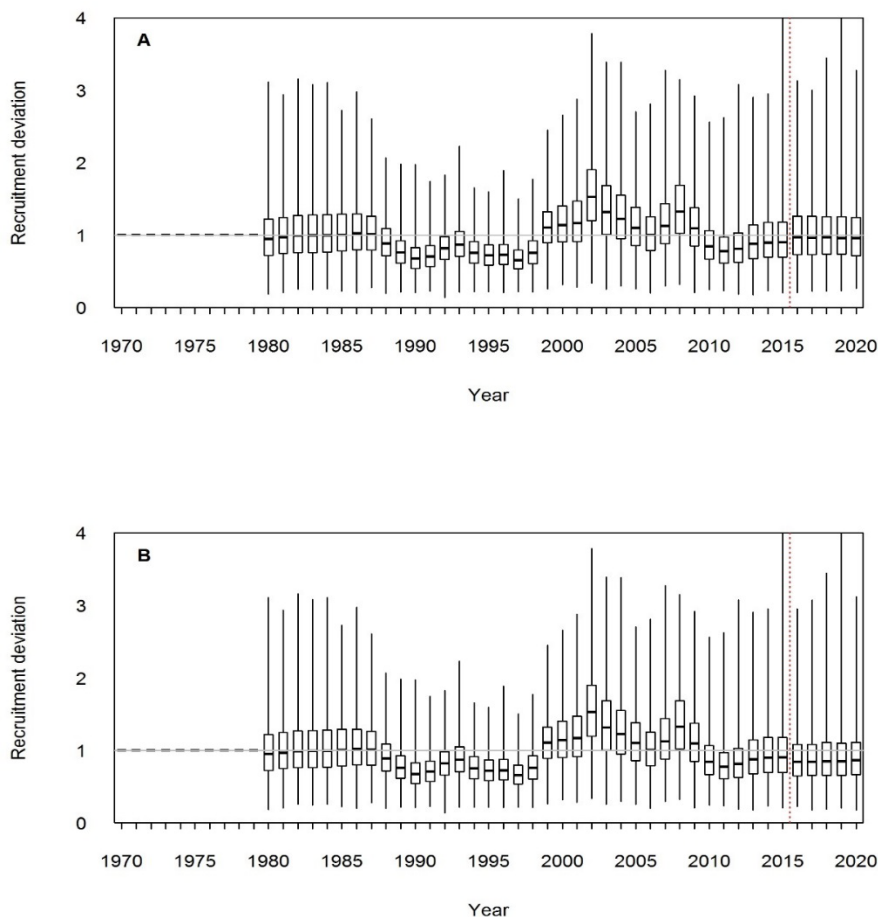


Figure 32: Recruitment year class multipliers around the stock recruitment relationship estimated and forecasted for model 0.1. The red line is the time where recruitment deviations were resampled for use in the projections. In panel A recruitments from the past ten years (2005–2015) were used for resampling, while in Panel B recruitments from the past five years (2011–2015) were used.

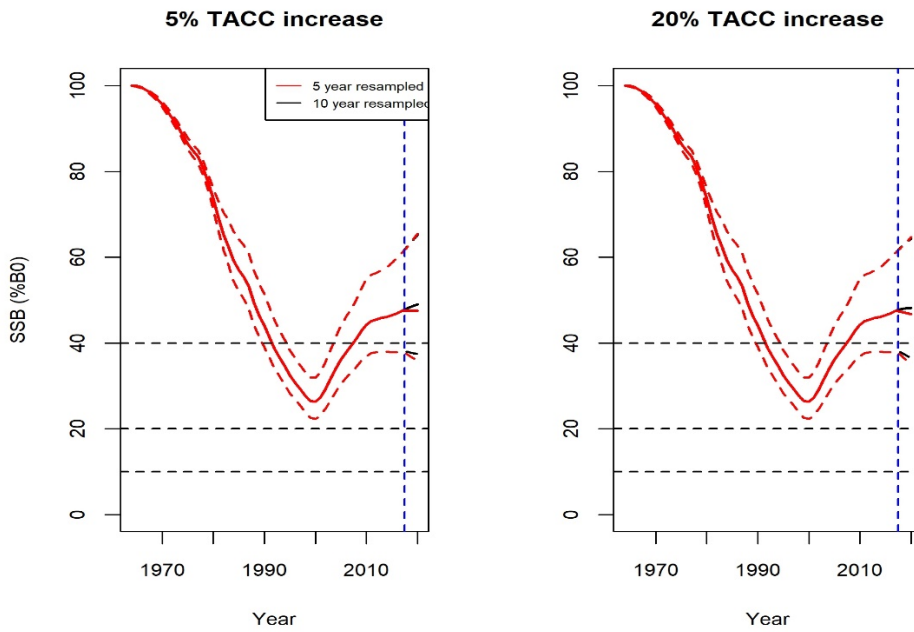


Figure 33: Median and 95% credible intervals of relative SSB from the base case model (0.1). This is shown for the two future recruitment scenarios and the lower (5%) and upper (20%) requested TACC change. The blue line separated the historic period (to the left) and the forecasted period (to the right).

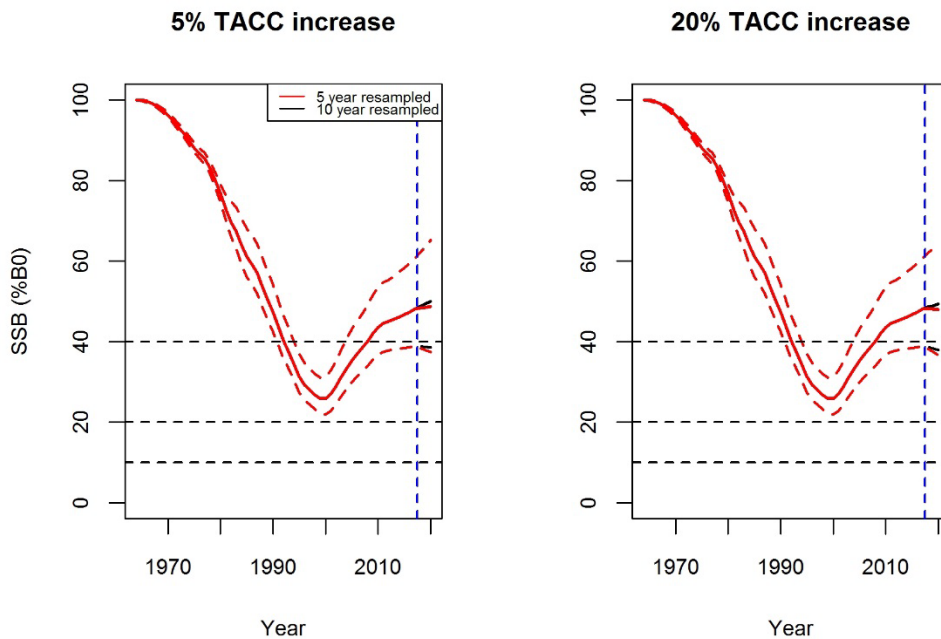


Figure 34: Median and 95% credible intervals of relative SSB from model 0.4. This is shown for the two future recruitment scenarios and the lower (5%) and upper (20%) requested TACC change. The blue line separated the historic period (to the left) and the forecasted period (to the right).

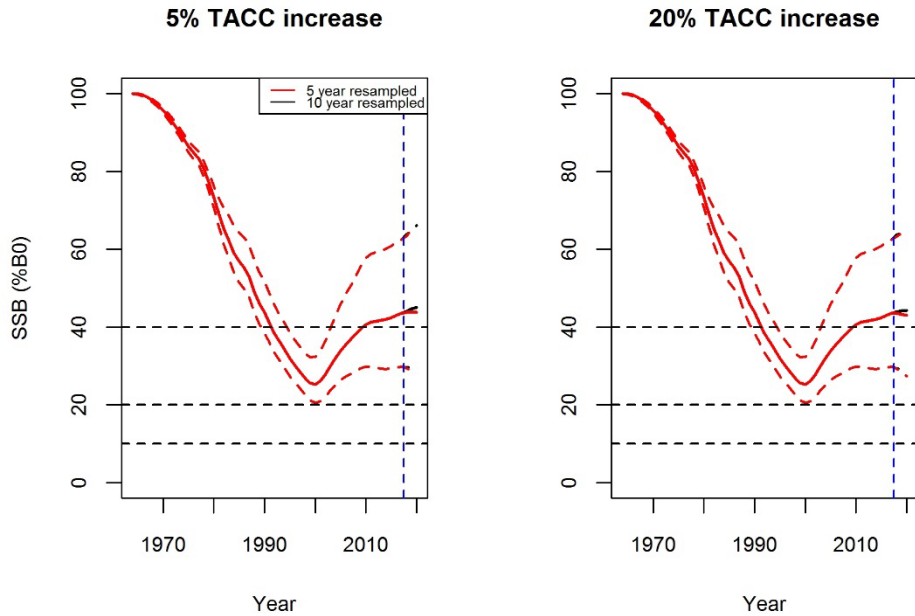


Figure 35: Median and 95% credible intervals of relative SSB from model 0.6. This is shown for the two future recruitment scenarios and the lower (5%) and upper (20%) requested TACC change. The blue line separated the historic period (to the left) and the forecast period (to the right).

Table 7: Projected quantities for the Base model with an assumed 5% TACC increase, and recruitment based on the past 10 years.

	2018	2019	2020
B_t	1898 (1460–2528)	1916 (1451–2594)	1936 (1439–2655)
$\%B_0$	0.48 (0.38–0.63)	0.49 (0.38–0.64)	0.49 (0.37–0.65)
$\%B_{msy}$	1.7 (1.4–2.2)	1.7 (1.4–2.3)	1.8 (1.3–2.3)
rB_t	1536 (1176–2031)	1550 (1176–2077)	1569 (1177–2124)
$\%rB_0$	0.43 (0.34–0.56)	0.44 (0.34–0.58)	0.44 (0.34–0.59)
$\%rB_{msy}$	2.0 (1.5–2.8)	2.0 (1.5–2.8)	2.0 (1.5–2.9)
$Pr (>B_{msy})$	1	1	1
$Pr (>B_{current})$	0.65	0.69	0.71
$Pr (>40\%B_0)$	0.93	0.93	0.93
$Pr (<20\%B_0)$	0	0	0
$Pr (<10\%B_0)$	0	0	0
$Pr (>rB_{msy})$	1	1	1
$Pr (>rB_{current})$	0.61	0.64	0.69
$Pr (U>U40\%B_0)$	0	0	0.01

Table 8: Projected quantities for the Base model with an assumed 20% TACC increase, and recruitment based on the past 10 years.

	2018	2019	2020
B_t	1892 (1453–2521)	1896 (1431–2574)	1904 (1407–2624)
%B₀	0.48 (0.38–0.62)	0.48 (0.37–0.63)	0.48 (0.37–0.64)
%B_{msy}	1.7 (1.4–2.2)	1.7 (1.3–2.2)	1.7 (1.3–2.3)
rB_t	1529 (1169–2024)	1530 (1156–2057)	1537 (1144–2092)
%rB₀	0.43 (0.34–0.56)	0.43 (0.33–0.57)	0.43 (0.33–0.58)
%rB_{msy}	2.0 (1.5–2.7)	2.0 (1.5–2.8)	2.0 (1.5–2.8)
Pr (>B_{msy})	1	1	1
Pr (>B_{current})	0.58	0.59	0.59
Pr (>40%B₀)	0.93	0.92	0.91
Pr (<20%B₀)	0	0	0
Pr (<10%B₀)	0	0	0
Pr (>rB_{msy})	1	1	1
Pr (>rB_{current})	0.53	0.51	0.53
Pr (U>U40%B₀)	0.02	0.02	0.03

Table 9: Projected quantities for the Base model with an assumed 5% TACC increase, and recruitment based on the past 5 years.

	2018	2019	2020
B_t	1876 (1434–2530)	1879 (1406–2571)	1876 (1373–2646)
%B₀	0.48 (0.37–0.62)	0.48 (0.37–0.64)	0.48 (0.36–0.65)
%B_{msy}	1.7 (1.3–2.2)	1.7 (1.3–2.3)	1.7 (1.3–2.3)
rB_t	1536 (1175–2032)	1545 (1167–2073)	1551 (1154–2119)
%rB₀	0.43 (0.34–0.56)	0.44 (0.34–0.58)	0.44 (0.33–0.59)
%rB_{msy}	2.0 (1.5–2.8)	2.0 (1.5–2.8)	2.0 (1.5–2.8)
Pr (>B_{msy})	1	1	1
Pr (>B_{current})	0.47	0.49	0.48
Pr (>40%B₀)	0.92	0.9	0.88
Pr (<20%B₀)	0	0	0
Pr (<10%B₀)	0	0	0
Pr (>rB_{msy})	1	1	1
Pr (>rB_{current})	0.6	0.6	0.59
Pr (U>U40%B₀)	0	0	0.01

Table 10: Projected quantities for the Base model with an assumed 20% TACC increase, and recruitment based on the past 5 years.

	2018	2019	2020
B_t	1869 (1427–2523)	1859 (1386–2551)	1844 (1341–2614)
%B₀	0.47 (0.37–0.62)	0.47 (0.36–0.63)	0.47 (0.35–0.65)
%B_{msy}	1.7 (1.3–2.2)	1.7 (1.3–2.2)	1.7 (1.3–2.3)
rB_t	1529 (1168–2025)	1525 (1147–2053)	1519 (1121–2087)
%rB₀	0.43 (0.34–0.56)	0.43 (0.33–0.57)	0.43 (0.32–0.58)
%rB_{msy}	2.0 (1.5–2.8)	2.0 (1.5–2.8)	2.0 (1.4–2.8)
Pr (>B_{msy})	1	1	1
Pr (>B_{current})	0.41	0.39	0.37
Pr (>40%B₀)	0.91	0.89	0.85
Pr (<20%B₀)	0	0	0
Pr (<10%B₀)	0	0	0
Pr (>rB_{msy})	1	1	1
Pr (>rB_{current})	0.52	0.48	0.44
Pr (U>U40%B₀)	0.02	0.02	0.03

Table 11: Projected quantities for model 0.4 (alternative catch history) with an assumed 5% TACC increase, and recruitment based on the past 10 years.

	2018	2019	2020
B_t	2173 (1689–2872)	2200 (1689–2926)	2231 (1686–2995)
%B₀	0.49 (0.39–0.62)	0.49 (0.39–0.64)	0.50 (0.39–0.65)
%B_{msy}	1.8 (1.4–2.2)	1.8 (1.4–2.3)	1.8 (1.4–2.3)
rB_t	1779 (1385–2322)	1804 (1385–2374)	1829 (1396–2422)
%rB₀	0.44 (0.35–0.57)	0.45 (0.35–0.58)	0.45 (0.35–0.59)
%rB_{msy}	2.0 (1.5–2.7)	2.1 (1.6–2.8)	2.1 (1.6–2.9)
Pr (>B_{msy})	1	1	1
Pr (>B_{current})	0.7	0.74	0.77
Pr (>40%B₀)	0.96	0.96	0.96
Pr (<20%B₀)	0	0	0
Pr (<10%B₀)	0	0	0
Pr (>rB_{msy})	1	1	1
Pr (>rB_{current})	0.72	0.75	0.79
Pr (U>U40%B₀)	0	0	0

Table 12: Projected quantities for model 0.4 (alternative catch history) with an assumed 20% TACC increase, and recruitment based on the past 10 years.

	2018	2019	2020
B_t	2166 (1682–2866)	2181 (1669–2907)	2199 (1654–2964)
%B₀	0.49 (0.39–0.62)	0.49 (0.38–0.63)	0.49 (0.38–0.64)
%B_{msy}	1.8 (1.4–2.2)	1.8 (1.4–2.3)	1.8 (1.4–2.3)
rB_t	1772 (1379–2315)	1784 (1365–2354)	1796 (1364–2390)
%rB₀	0.44 (0.35–0.56)	0.44 (0.35–0.57)	0.45 (0.35–0.58)
%rB_{msy}	2.0 (1.5–2.7)	2.0 (1.5–2.8)	2.0 (1.5–2.8)
Pr (>B_{msy})	1	1	1
Pr (>B_{current})	0.65	0.65	0.66
Pr (>40%B₀)	0.95	0.95	0.94
Pr (<20%B₀)	0	0	0
Pr (<10%B₀)	0	0	0
Pr (>rB_{msy})	1	1	1
Pr (>rB_{current})	0.64	0.63	0.66
Pr (U>U40%B₀)	0	0	0

Table 13: Projected quantities for model 0.4 (alternative catch history) with an assumed 5% TACC increase, and recruitment based on the past 5 years.

	2018	2019	2020
B_t	2159 (1668–2877)	2172 (1646–2952)	2177 (1620–3024)
%B₀	0.48 (0.38–0.62)	0.49 (0.38–0.63)	0.49 (0.37–0.65)
%B_{msy}	1.7 (1.4–2.2)	1.7 (1.4–2.3)	1.8 (1.3–2.3)
rB_t	1778 (1385–2322)	1802 (1382–2378)	1818 (1376–2441)
%rB₀	0.44 (0.35–0.57)	0.45 (0.35–0.58)	0.45 (0.35–0.59)
%rB_{msy}	2.0 (1.6–2.7)	2.1 (1.5–2.8)	2.1 (1.5–2.9)
Pr (>B_{msy})	1	1	1
Pr (>B_{current})	0.57	0.58	0.58
Pr (>40%B₀)	0.94	0.94	0.92
Pr (<20%B₀)	0	0	0
Pr (<10%B₀)	0	0	0
Pr (>rB_{msy})	1	1	1
Pr (>rB_{current})	0.71	0.72	0.71
Pr (U>U40%B₀)	0	0	0

Table 14: Projected quantities for model 0.4 (alternative catch history) with an assumed 20% TACC increase, and recruitment based on the past 5 years.

	2018	2019	2020
B_t	2153 (1661–2871)	2152 (1626–2932)	2145 (1587–2992)
%B₀	0.48 (0.38–0.62)	0.48 (0.38–0.63)	0.48 (0.37–0.64)
%B_{msy}	1.7 (1.4–2.2)	1.7 (1.3–2.3)	1.7 (1.3–2.3)
rB_t	1772 (1378–2315)	1782 (1362–2358)	1785 (1343–2409)
%rB₀	0.44 (0.35–0.56)	0.44 (0.35–0.57)	0.44 (0.34–0.58)
%rB_{msy}	2.0 (1.5–2.7)	2.0 (1.5–2.8)	2.0 (1.5–2.8)
Pr (>B_{msy})	1	1	1
Pr (>B_{current})	0.51	0.48	0.47
Pr (>40%B₀)	0.94	0.92	0.9
Pr (<20%B₀)	0	0	0
Pr (<10%B₀)	0	0	0
Pr (>rB_{msy})	1	1	1
Pr (>rB_{current})	0.63	0.6	0.58
Pr (U>U40%B₀)	0	0	0

Table 15: Projected quantities for model 0.6 (time varying catchability) with an assumed 5% TACC increase, and recruitment based on the past 10 years.

	2018	2019	2020
B_t	1729 (1141–2660)	1749 (1130–2692)	1766 (1124–2730)
%B₀	0.44 (0.30–0.64)	0.45 (0.30–0.65)	0.45 (0.30–0.66)
%B_{msy}	1.6 (1.1–2.3)	1.6 (1.1–2.3)	1.6 (1.1–2.4)
rB_t	1393 (898–2151)	1409 (892–2191)	1426 (899–2207)
%rB₀	0.39 (0.26–0.58)	0.40 (0.26–0.59)	0.40 (0.26–0.60)
%rB_{msy}	1.8 (1.1–2.9)	1.8 (1.1–2.9)	1.8 (1.1–2.9)
Pr (>B_{msy})	0.99	0.99	0.98
Pr (>B_{current})	0.64	0.67	0.7
Pr (>40%B₀)	0.69	0.7	0.71
Pr (<20%B₀)	0	0	0
Pr (<10%B₀)	0	0	0
Pr (>rB_{msy})	0.99	0.99	0.99
Pr (>rB_{current})	0.64	0.67	0.71
Pr (U>U40%B₀)	0.13	0.14	0.13

Table 16: Projected quantities for model 0.6 (time varying catchability) with an assumed 20% TACC increase, and recruitment based on the past 10 years.

	2018	2019	2020
B_t	1722 (1134–2654)	1729 (1110–2672)	1734 (1091–2698)
%B₀	0.44 (0.29–0.64)	0.44 (0.29–0.64)	0.44 (0.29–0.65)
%B_{msy}	1.6 (1.1–2.3)	1.6 (1.0–2.3)	1.6 (1.0–2.3)
rB_t	1387 (891–2144)	1389 (872–2171)	1394 (865–2176)
%rB₀	0.39 (0.25–0.58)	0.39 (0.25–0.59)	0.39 (0.25–0.60)
%rB_{msy}	1.8 (1.1–2.8)	1.8 (1.1–2.9)	1.8 (1.1–2.9)
Pr (>B_{msy})	0.99	0.98	0.98
Pr (>B_{current})	0.57	0.56	0.56
Pr (>40%B₀)	0.68	0.68	0.68
Pr (<20%B₀)	0	0	0
Pr (<10%B₀)	0	0	0
Pr (>rB_{msy})	0.99	0.99	0.98
Pr (>rB_{current})	0.56	0.52	0.54
Pr (U>U40%B₀)	0.23	0.24	0.25

Table 17: Projected quantities for model 0.6 (time varying catchability) with an assumed 5% TACC increase, and recruitment based on the past 5 years.

	2018	2019	2020
B_t	1716 (1120–2656)	1721 (1099–2674)	1720 (1079–2733)
%B₀	0.44 (0.29–0.63)	0.44 (0.29–0.65)	0.44 (0.28–0.66)
%B_{msy}	1.6 (1.1–2.3)	1.6 (1.0–2.3)	1.6 (1.0–2.3)
rB_t	1393 (898–2152)	1405 (892–2187)	1417 (880–2207)
%rB₀	0.39 (0.26–0.58)	0.40 (0.26–0.59)	0.40 (0.25–0.60)
%rB_{msy}	1.8 (1.1–2.9)	1.8 (1.1–2.9)	1.8 (1.1–2.9)
Pr (>B_{msy})	0.98	0.98	0.98
Pr (>B_{current})	0.5	0.51	0.5
Pr (>40%B₀)	0.67	0.67	0.67
Pr (<20%B₀)	0	0	0
Pr (<10%B₀)	0	0	0
Pr (>rB_{msy})	0.99	0.99	0.99
Pr (>rB_{current})	0.64	0.64	0.63
Pr (U>U40%B₀)	0.13	0.14	0.13

Table 18: Projected quantities for model 0.6 (time varying catchability) with an assumed 20% TACC increase, and recruitment based on the past 5 years.

	2018	2019	2020
B_t	1709 (1113–2649)	1701 (1079–2654)	1687 (1045–2701)
%B₀	0.44 (0.29–0.63)	0.43 (0.28–0.64)	0.43 (0.27–0.65)
%B_{msy}	1.6 (1.0–2.3)	1.6 (1.0–2.3)	1.54 (0.98–2.32)
rB_t	1386 (891–2145)	1385 (872–2167)	1384 (847–2176)
%rB₀	0.39 (0.25–0.58)	0.39 (0.25–0.58)	0.39 (0.24–0.59)
%rB_{msy}	1.8 (1.1–2.9)	1.8 (1.1–2.9)	1.8 (1.0–2.9)
Pr (>B_{msy})	0.98	0.98	0.97
Pr (>B_{current})	0.44	0.4	0.38
Pr (>40%B₀)	0.66	0.65	0.63
Pr (<20%B₀)	0	0	0
Pr (<10%B₀)	0	0	0
Pr (>rB_{msy})	0.99	0.99	0.98
Pr (>rB_{current})	0.55	0.5	0.47
Pr (U>U40%B₀)	0.24	0.25	0.26

A. APPENDIX A

Appendix A: Summary of results for MPD model runs

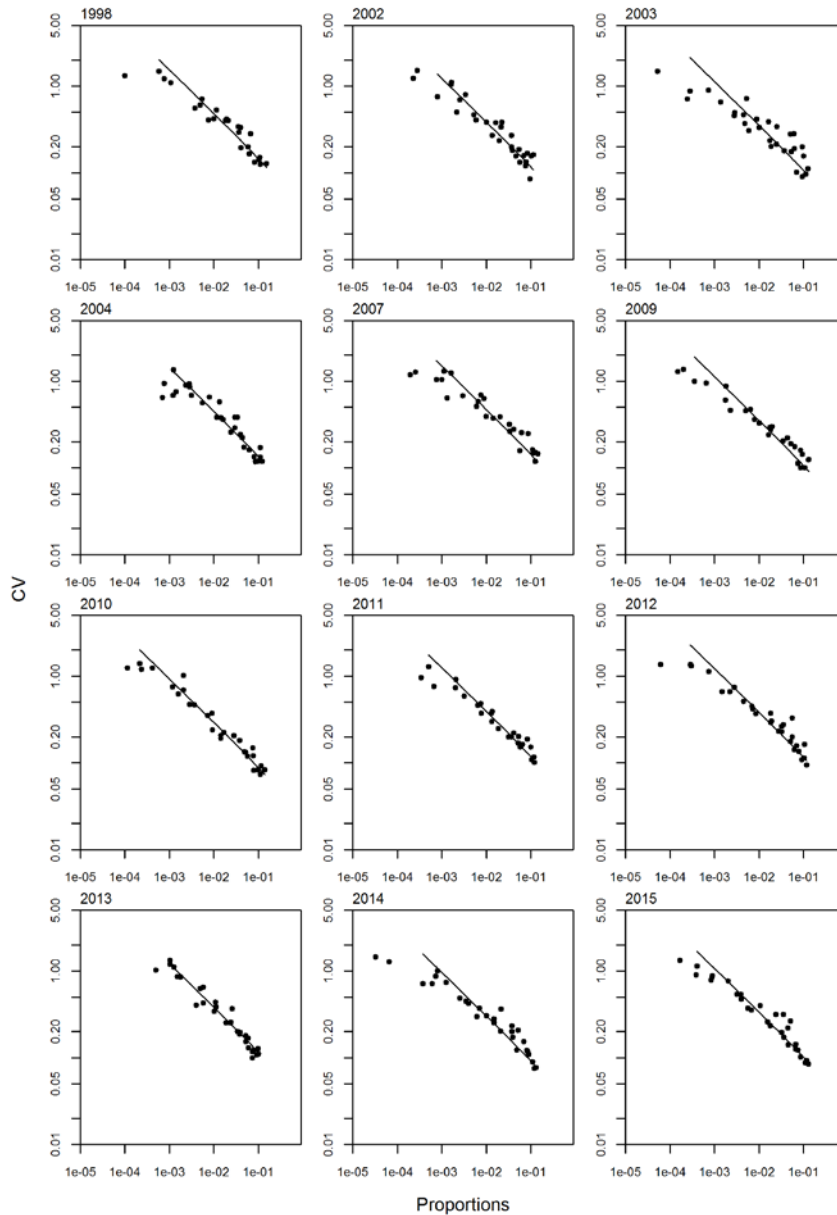


Figure A1: Estimated proportions versus CVs for the commercial catch length frequencies for PAU 5B. Lines indicate the best least squares fit for the effective sample size of the multinomial distribution.

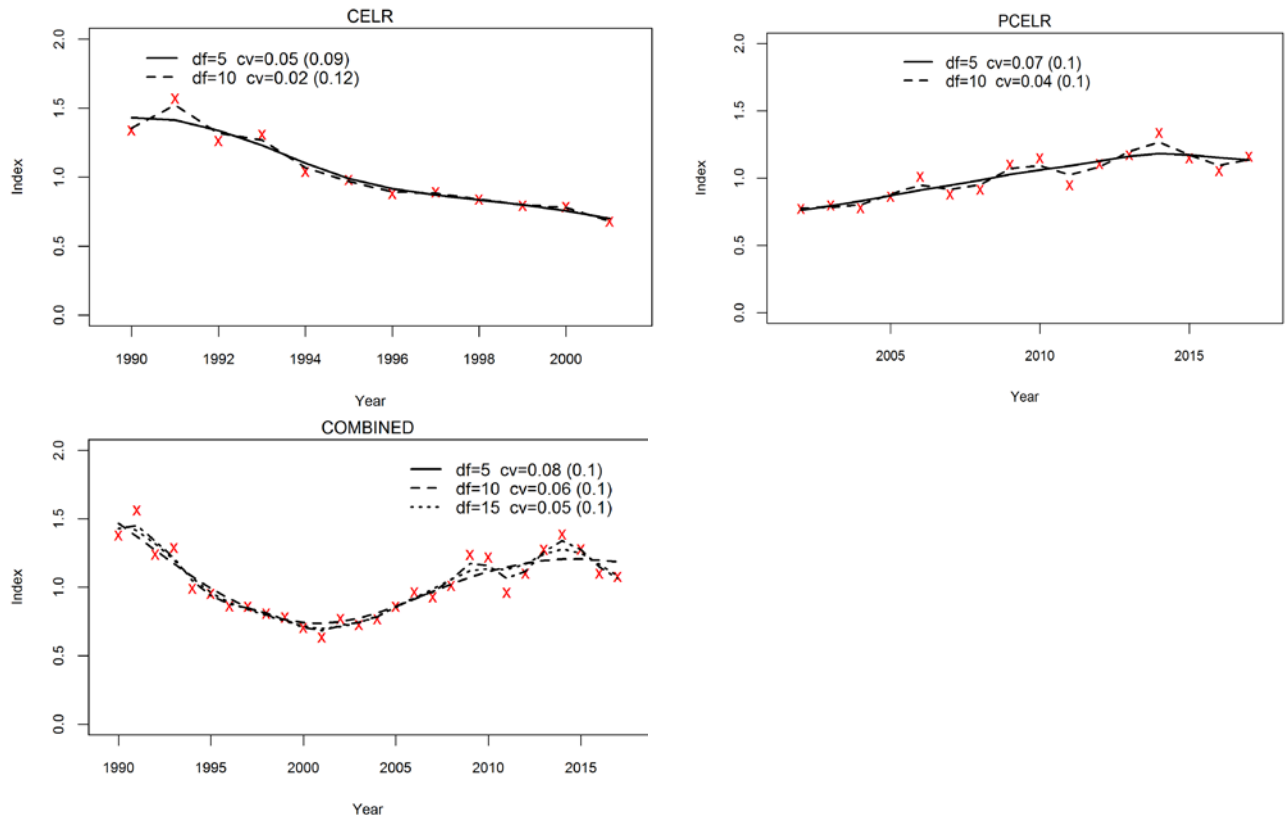


Figure A2: A series of lowess lines of various degrees of freedom (df) fitted to the PAU 5B standardised CPUE indices for 1990–2001 (top-left), 2002–2017 (top-right) and combined series 1990-2017 (bottom left). CVs are calculated from residuals for each of the fitted lowess line and are further adjusted for the degree of “smoothing” (adjusted value in the bracket). The CV of from the “appropriate” fit will be used as the CV in the stock assessment model. What is "appropriate" is judged by the SFWG by visual examination of lines with different degrees of smoothing.

GLOSSARY

This glossary is aimed at making this document more accessible to non-technical readers. A knowledge of statistical terms is assumed and such terms are not explained here. Technical terms are defined with specific reference to the paua stock assessment and may not be applicable in other contexts.

abundance index: usually a time-series of relative estimates of abundance in numbers or weight (biomass)

Bayesian stock assessment: an inferential method that allows prior information or expert judgement to be used formally in addition to the data. Often uncertainty is estimated using Markov chain Monte Carlo simulations (MCMC) which samples the posterior distribution of estimated and derived parameters.

bounds: model parameters can be restricted so that parameter estimates cannot be less than a lower bound or higher than an upper bound; these are sometimes necessary to prevent mathematical impossibility (e.g. a proportion must be between 0 and 1 inclusive) or to ensure biologically realistic model results.

catchability: a proportionality constant that relates a relative abundance index, such as CPUE, to absolute biomass; usually has the symbol q .

CELRL: A standardised CPUE series covering 1990–2001 based on catch effort landing return data.

CSLF: A commercial catch sampling length frequency series

CPUE: catch per unit of effort; usually has the units kg of catch per trip; assumed to be a relative abundance index such that $CPUE = catchability \times vulnerable\ biomass$; can be estimated in several ways (see standardisation).

derived parameter: any quantity that depends on the model’s estimated parameters; e.g. average recruitment (R_0) is an estimated parameter but initial biomass (B_0) is a derived parameter that is determined by model parameters for growth, natural mortality and recruitment.

equilibrium: in models, a stable state that is reached when catch, fishing patterns, recruitment and other biological processes are constant; does not occur in nature.

exploitation rate: a measure of fishing intensity; catch in a year or period divided by initial biomass; symbol U

fixed parameter: a parameter that could be estimated by the model but that is forced to remain at the specified initial value.

initial value: when the model minimises, it has to start with a parameter set and the initial values comprise this set.

length frequency (LF) (also called size frequency): The distribution of numbers-at-size (TW) from catch samples; based either on observer catch sampling or voluntary logbooks; the raw data are compiled with a complex weighting procedure.

MCMC: Markov chain Monte Carlo simulations. MCMC simulations explore the combinations of parameters in the region near the “best” set of parameters, and from this set, the uncertainty in estimated and derived parameters can be measured. In one “simulation”, the algorithm generates a new parameter set, calculates the function value and chooses whether to accept or reject the new point.

MLS: Minimum legal size.

MHS: Minimum Harvest size.

MSY: under the MSY paradigm, the maximum average catch that can be taken sustainably from the stock under constant environmental conditions; usually calculated under simplistic assumptions.

natural mortality: (symbol M) the instantaneous rate of mortality from natural causes. If there were no fishing mortality F , survival would be e^{-M} .

normalised residual: the residual divided by the standard deviation of observation error that is assumed or estimated in the minimising procedure.

PCELR: A standardised CPUE series covering 2002–2017 based on Paua catch effort landing return.

priors: short for prior probability distribution; these allow the modeller to estimate parameter values using Bayes's theorem and (if desired) to incorporate prior belief (based on data that are not being used by the model) about any likely parameter values.

RDLF: Research diver length frequency

RDSI: Research diver survey index, a dataset that represents fishery independent measure of relative biomass.

recruitment: can mean recruitment to the population (as in puerulus settlement), recruitment to the model at a specified size, or recruitment to the stock (by growing above MLS); when used with no qualification in documentation here it means “recruitment to the model”.

resampling: in projections, recruitment for a projection year is equal to estimated recruitment in a randomly chosen year that lies within the range of years being resampled.

residual: the observed data value minus the model's predicted value, for instance for CPUE in a given time step it would be the difference between the observed CPUE in that year and the model's predicted value.

SDNR: the standard deviation of normalised residuals; in a good estimation with multiple data sets, this should be close to 1; a common procedure is to weight datasets to try to obtain SDNRs close to 1.

SFWG: The shellfish working group. Throughout this assessment process, multiple working groups were conducted to peer review the work and decision making process. These are attended by experts in the field.

selectivity: selectivity describes the relative chance of a paua being caught, given its sex and size, hence “selectivity ogive”, generally driven by minimum legal sizes.

sensitivity run: a base case stock assessment model is the result of inevitable choices made by the modeller; sensitivity trials examine whether results are seriously dependent on (“sensitive to”) these choices.

standardisation: a statistical procedure that extracts patterns in catch and effort data associated with explanatory variables; the pattern in the time variable (e.g. period or year) is interpreted as an abundance index.

stock: by definition, a group of fish inhabiting a quota management area QMA; may often not coincide with biological population definitions.

TAC: Total Allowable Catch limit set by the Minister for Primary Industries for a stock.

TACC: Total Allowable Commercial Catch limit set by the Minister for Primary Industries for a stock.